

1 Future snowfall in the Alps: Projections based on the EURO- 2 CORDEX regional climate models

3 Prisco Frei, Sven Kotlarski, Mark A. Liniger, Christoph Schär

6 - Response to Referees –

8 General

9 We thank the three referees for their careful revision of the manuscript and for their constructive comments.
10 Please find below our replies to all major comments and our suggestions on how to address these issues in a
11 revised manuscript. We hope that we satisfactorily addressed all referee comments and that the proposed
12 changes are considered as being appropriate. In case that not, we'd be looking forward to discuss individual
13 remaining issues in more detail.

14 As several referee comments addressed the RCM evaluation and the evaluation of the 2 km snowfall reference
15 itself, we'd like to put in front the following two statements on the scope of the paper:

16
17 (1) Our work is primarily concerned with the analysis of future snowfall projections. However, a basic notion on
18 the quality of raw RCM snowfall and, hence, the general ability of RCMs to represent our variable of interest is
19 required for such an exercise in our opinion. In the manuscript this is accomplished by comparing RCM raw
20 snowfall against site-scale measurements obtained from new snow sums (Figure 3). Such a comparison is
21 subject to considerable uncertainties, mostly originating from the scale gap between RCM grid cells and site-scale
22 observations and from representativity issues of observed snow cover. Due to a missing high-quality
23 observational reference at the scale of the RCM resolution (in our opinion also the HISTALP dataset has its
24 shortcomings; see below) we refrain from evaluating RCM snowfall in more detail and, at least when interpreting
25 raw snowfall change signals, implicitly assume stationary model biases. As a consequence, the projection aspect
26 of the current work is much larger than the evaluation aspect, and we tried to better clarify this issue by modifying
27 the text in Chapters 1 and 3.1. Furthermore, we adjusted the title of the manuscript accordingly and removed the
28 term "Evaluation".

29
30 (2) Relating to the previous issue but especially to the validation of the snowfall reference against which the RCM-
31 derived snowfall is adjusted: As it was already mentioned in the introduction of the original manuscript, we do not
32 claim to present an ultimate solution for bias-adjusting RCM-based snowfall but employ a spatially and temporally
33 aggregated adjustment procedure that does nevertheless separately account for temperature and precipitation
34 biases. Aspects of the snowfall climate that are not corrected for, such as details of the spatial snowfall pattern,
35 are described in Sections 2.6 and 3.3. The simplifications also include the fact that we basically accept a non-
36 perfect observation-based reference. A well-validated and appropriate reference does not exist in our opinion (see
37 also above). The very core of our work is the analysis of projected future snowfall changes and the comparison of
38 three different ways to produce such estimates: (1) Raw RCM snowfall, (2) RCM snowfall as separated from
39 simulated temperature and precipitation, and (3) RCM snowfall as separated from simulated temperature and
40 precipitation and additionally bias-adjusted. The latter version is the basic dataset for the climate scenario
41 analysis as it can be constructed for all participating RCMs (raw snowfall is not available for all of them) and as it
42 is, in principle, able to account for temperature-dependent and hence non-stationary snowfall biases. However,
43 Chapter 5.3 shows that relative change estimates largely agree among all three datasets and are robust. From
44 that point of view, the influence of remaining inaccuracies in the bias-adjusted snowfall projections due to
45 inaccuracies of the reference is presumably small. In the revised version we now try to better clarify these issues
46 by modifying Chapters 1, 2.5, 2.6 and 5.3.

47 Response to Referee #1

48 **Comment L. 65-66:** replace "the GCM provides the lateral boundary conditions to the RCM" with "the GCM provides the lateral and sea surface
49 boundary conditions to the RCM".

50 **Response and changes to manuscript** Modified accordingly.

51 **Comment L. 88-89:** the fact that "a gridded observational snowfall product that could serve as reference for RCM evaluation does not exist" is not
52 a good reason for not using raw outputs, it can actually be evaluated as in Fig. 13 of this paper:

53 **Response and changes to manuscript** You are perfectly right, thanks very much for pointing this out. The
54 reason is indeed the non-availability of raw snowfall output in several experiments. We removed the second part
55 of this sentence.

56 **Comment L. 133-135:** the RCMs also have an effective resolution that is larger than their grid resolution, see e.g. Skamarock et al. (Mon. Wea.
57 Rev. 2004), Lefèvre et al. (Mar. Pol. Bull. 2010).

58 **Response and changes to manuscript** Thanks for pointing this out. We now use the term “nominal resolution of
59 the available climate model data”, but would like to refrain from further discussing the even coarser effective
60 resolution of climate models as we believe that this would distract the reader at this point.

61 **Comment L. 151:** the authors should make clear that what they refer to as “control” is based on the CMIP5 historical simulations (not the one
62 based on reanalyses).

63 **Response and changes to manuscript** The fact that GCM-driven experiments are employed has already been
64 mentioned several times in the respective paragraph. We slightly revised this paragraph now to make this point
65 even clearer.

66 **Comment Section 2.2:** it is worth mentioning that daily-averages from EURO-CORDEX are used (or specify what other time sampling/averaging is
67 used).

68 **Response and changes to manuscript** This point is mentioned now.

69 **Comment Fig. 1:** which topography is shown?

70 **Response and changes to manuscript** Thanks for this comment, this information was indeed missing so far.
71 The topography shown is the GTOPO30 digital elevation model of the U.S. Geological Survey. The figure caption
72 was adjusted accordingly. As GTOPO30 is also the basis for computing the topographical standard deviation σ_h
73 for each RCM grid cell in the course of calibrating the Richards method we furthermore provide this information
74 now in Section 2.5 of the manuscript and also added one sentence to the acknowledgments.

75 **Comment L.246-249:** it is not clear to me why the explanation cannot be reversed: coarse cells with grid temperature lower than T^* should
76 overestimate snowfall at some locations covered by the cell, don't they? If it's not zero on average, is it because elevation distribution is generally
77 skewed within the coarse cell?

78 **Response and changes to manuscript** A skewed subgrid topography distribution might be one reason, but the
79 main factor is probably the fact that precipitation-elevation gradients over many parts of the analysis domain are
80 positive, i.e. higher total precipitation sums at higher (=colder) elevations. Snowfall separation on the high-
81 resolution grid would therefore lead to higher spatially-averaged mean snowfall sums compared to the coarse-
82 resolution version, hence a systematic non-zero difference of the two versions. We modified the respective text
83 section in order to better clarify this point.

84 **Comment L. 463:** I think that “Rhone Valley” would be more appropriate than “Western France”.

85 **Response and changes to manuscript** Thanks a lot, we modified this sentence accordingly.

86 **Comment L. 485:** typo “change sin”.

87 **Response and changes to manuscript** Corrected.

88 **Comment Fig. 11:** indicate what the grey area represents.

89 **Response and changes to manuscript** We're sorry, this information was mentioned in the text but not in the
90 figure caption so far. The grey area represents the overall temperature interval at which snowfall occurs (light
91 grey) as well as the preferred temperature interval for heavy snowfall to occur (dark grey). This information has
92 been added to the figure caption now.

93 **Comment Section 5.3:** that relative changes in snowfall from raw model outputs are very similar to separated and bias-corrected fields is a very
94 interesting finding and should definitely be reported in the Abstract.

95 **Response and changes to manuscript** You are perfectly right, thanks for pointing this out. One sentence on this
96 finding has now been added to the abstract.

97 **Comment L.656-658:** It is indeed a pity that no evaluation is performed based on datasets from other alpine countries. It would also help validate
98 the overall methodology since the methods tuning is undertaken over the Swiss Alps.

99 **Response and changes to manuscript** Following a suggestion of Referee #2 an additional comparison of the
100 constructed reference snowfall against the HISTALP dataset has been added to the manuscript. Please see our
101 replies to Referee #2 and Figure S5 of the revised manuscript. Please also see our general replies above
102 concerning the importance of an accurate reference in the context of our study.

103

104 **Further changes to the manuscript**

105 **Chapter 2.1 “Observational data”** For reasons of completeness we additionally included the information that the
106 temperature and precipitation grids employed are slightly shifted with respect to their reference time interval
107 (midnight UTC - midnight UTC for temperature, 06 UTC - 06 UTC for precipitation).

108 **Chapter 2.2 “Climate model data”** In the last paragraph we erroneously spoke of *six* RCMs considered. We
109 corrected this to *seven* RCMs.

110 **Chapter 3.1** To better account for uncertainties in this simplified evaluation we now additionally cite the work of
111 Grünewald and Lehning (2015) that highlights the danger of non-representativity of single-site snow depth
112 observations in Alpine terrain.

113 **Figure 3** In the left panel two of the 29 stations employed (WFJ and MVE) were plotted at a wrong elevation in
114 the original version. For both stations the correct elevation differs by about 100 m from the previously used
115 elevation. The figure has been corrected accordingly, in addition to the modifications to this figure mentioned
116 above. The conclusions of the analysis do not change.

117 **Overall manuscript** Several minor spelling and wording mistakes as well as an inconsistent use of past and
118 present tense were corrected.

119
120

121

122

Future sSnowfall in the Alps: ~~Evaluation~~ and pProjections based on the EURO-CORDEX regional climate models

Prisco Frei¹, Sven Kotlarski^{2,*}, Mark A. Liniger², Christoph Schär¹

¹ Institute for Atmospheric and Climate Sciences, ETH Zurich, [CH-8006](#), Zurich, Switzerland

² Federal Office of Meteorology and Climatology, MeteoSwiss, [CH-8058](#) Zurich-Airport, Switzerland

* Corresponding author: sven.kotlarski@meteoswiss.ch

Abstract. Twenty-first century snowfall changes over the European Alps are assessed based on high-resolution regional climate model (RCM) data made available through the EURO-CORDEX initiative. Fourteen different combinations of global and regional climate models with a target resolution of 12 km, and two different emission scenarios are considered. As raw snowfall amounts are not provided by all RCMs, a newly developed method to separate snowfall from total precipitation based on near-surface temperature conditions and accounting for subgrid-scale topographic variability is employed. The evaluation of the simulated snowfall amounts against an observation-based reference indicates the ability of RCMs to capture the main characteristics of the snowfall seasonal cycle and its elevation dependency, but also reveals considerable positive biases especially at high elevations. These biases can partly be removed by the application of a dedicated RCM bias ~~correction~~ adjustment that separately considers temperature and precipitation biases.

Snowfall projections reveal a robust signal of decreasing snowfall amounts over most parts of the Alps for both emission scenarios. Domain and multi-model -mean decreases of mean September-May snowfall by the end of the century amount to -25% and -45% for RCP4.5 and RCP8.5, respectively. Snowfall in low-lying areas in the Alpine forelands could be reduced by more than -80%. These decreases are driven by the projected warming and are strongly connected to an important decrease of snowfall frequency and snowfall fraction and are also apparent for heavy snowfall events. In contrast, high-elevation regions could experience slight snowfall increases in mid-winter for both emission scenarios despite the general decrease of the snowfall fraction. These increases in mean and heavy snowfall can be explained by a general increase of winter precipitation and by the fact that, with increasing temperatures, climatologically cold areas are shifted into a temperature interval which favours higher snowfall intensities. In general, percentage changes of snowfall indices are robust with respect to the RCM postprocessing strategy employed: Similar results are obtained for raw, separated and separated + bias-adjusted snowfall amounts. Absolute changes, however, can differ among these three methods.

161 1 Introduction

162 Snow is an important resource for the Alpine regions, be it for tourism, hydropower generation, or
163 water management (Abegg et al., 2007). According to the Swiss Federal Office of Energy (SFOE)
164 hydropower generation accounts for approximately 55% of the Swiss electricity production (SFOE,
165 2014). Consideration of changes in snow climatology needs to address aspects of both snow cover
166 and snow-fall. In the recent past, an important decrease of the mean snow cover depth and duration in
167 the Alps was observed (e.g, Laternser and Schneebeli, 2003; Marty, 2008; Scherrer et al., 2004).
168 ~~Future p~~Projections of future snow cover changes based on using climate model simulations ~~of the~~
169 ~~anthropogenic greenhouse effect~~ indicate a further substantial reduction (Schmucki et al., 2015a;
170 Steger et al., 2013), strongly linked to the expected rise of temperatures (e.g., CH2011, 2011; Gobiet
171 et al., 2014). On regional and local scales rising temperatures exert a direct influence on snow cover in
172 two ways: First, total snowfall sums are expected to decrease by a ~~decreasing-lower~~ probability for
173 precipitation to fall as snow implying and a decreasing snowfall fraction (ratio between solid and total
174 precipitation). Second, snow on the ground is subject to faster and accelerated melt. These warming-
175 induced trends might be modulated by changes in atmospheric circulation statistics~~patterns~~.

176 Although the snowfall fraction is expected to decrease ~~at lower elevations~~ during the 21st century
177 (e.g., Räisänen, 2016), extraordinary snowfall events can still leave a trail of destruction. A recent
178 example was the winter 2013/2014 with record-breaking heavy snowfall events along the southern rim
179 of the European Alps (e.g., Techel et al., 2015). The catastrophic effects of heavy snowfall range from
180 avalanches and floods to road or rail damage. In extreme cases these events can even result in the
181 weight-driven collapse of buildings or loss of human life (Marty and Blanchet, 2011). Also mean
182 snowfall conditions, such as the mean number of snowfall days in a given period, can be of high
183 relevance for road management (e.g. Zubler et al., 2015) or airport operation. Projections of future
184 changes in ~~the snowfall-climate~~, including mean and extreme conditions, are therefore highly relevant
185 for long-term planning and adaptation purposes in order to assess and prevent related socio-economic
186 impacts and costs.

187 21st century climate projections typically rely on climate models. For large-scale projections, global
188 climate models (GCMs) with a rather coarse spatial resolution of 100 km or more are used. ~~For~~
189 assessing~~To assess~~ regional to local scale impacts, where typically a much higher spatial resolution
190 ~~of the projections~~ is required, a GCM can be dynamically downscaled by nesting a regional climate
191 model (RCM) over the specific domain of interest (Giorgi, 1990). In such a setup, the GCM provides
192 the lateral and sea surface boundary conditions to the RCM. One advantage of climate models is the
193 ability to estimate climate change in a physically based manner under different greenhouse gas (GHG)
194 emission scenarios. With the Intergovernmental Panel on Climate Change's (IPCC) release of the Fifth
195 Assessment Report (AR5; IPCC, 2013) the so-called representative concentration pathway (RCP)
196 scenarios have been introduced (Moss et al., 2010) which specify GHG concentrations and
197 corresponding emission pathways for several radiative forcing targets. To estimate inherent projection
198 uncertainties, ensemble approaches employing different climate models, different greenhouse gas
199 scenarios, and/or different initial conditions are being used (e.g., Deser et al., 2012; Hawkins and
200 Sutton, 2009; Rummukainen, 2010).

201 Within the last few years several studies targeting the future global and European snowfall evolution
202 based on climate model ensembles were carried out (e.g., de Vries et al., 2013; de Vries et al., 2014;
203 Krasting et al., 2013; O’Gorman, 2014; Piazza et al., 2014; Räisänen, 2016; Soncini and Bocchiola,
204 2011). Most of these analyses are based on GCM output or older generations of RCM ensembles at
205 comparatively low spatial resolution, which are not able to properly resolve snowfall events over
206 regions with complex topography. New generations of high resolution RCMs are a first step toward an
207 improvement on this issue. This is in particular true for the most recent high-resolution regional climate
208 change scenarios produced by the global CORDEX initiative (Giorgi et al., 2009) and its European
209 branch EURO-CORDEX (Jacob et al., 2014). The present work aims to exploit this recently
210 established RCM archive with respect to future snowfall conditions over the area of the European
211 Alps. It thereby complements the existing works of Piazza et al. (2014) and de Vries et al. (2014) who
212 among others also exploit comparatively high-resolved RCM experiments (partly originating from
213 EURO-CORDEX as well) but with a reduced ensemble size and/or not specifically targeting the entire
214 Alpine region.

215 In general and on decadal to centennial time scales, two main drivers of future snowfall changes over
216 the European Alps with competing effects on snowfall amounts are apparent from the available
217 literature: (1) Mean winter precipitation is expected to increase over most parts of the European Alps
218 and in most EURO-CORDEX experiments (e.g., Rajczak et al., in prep.; Smiatek et al., 2016) which in
219 principle could lead to higher snowfall amounts. (2) Temperatures are projected to considerably rise
220 throughout the annual cycle (e.g., Gobiet et al., 2014; Smiatek et al., 2016; Steger et al., 2013) with
221 the general effect of a decreasing snowfall frequency and fraction, thus potentially leading to a
222 reduction in overall snowfall amounts. Separating the above two competing factors is one of the
223 targets of the current study. A potential complication is that changes in daily precipitation frequency
224 (here events with precipitation > 1 mm/day) and precipitation intensity (average amount on wet days)
225 can change in a counteracting manner (e.g., Fischer et al., 2015; Rajczak et al., 2013), and that
226 relative changes are not uniform across the event category (e.g. Ban et al., 2015; Fischer and Knutti,
227 2016).

228 We here try to shed more light on these issues by addressing the ~~By covering both model evaluation~~
229 ~~and high-resolution future snowfall projections we are addressing the~~ following main objectives:

230 **Snowfall separation on an ~~(coarse resolution)~~ RCM grid.** Raw snowfall outputs are not available
231 for all members of the EURO-CORDEX RCM ensemble ~~and, furthermore, a gridded observational~~
232 ~~snowfall product that could serve as reference for RCM evaluation does not exist.~~ Therefore, an
233 adequate snowfall separation technique, i.e., the derivation of snowfall amounts based on readily
234 available daily near-surface air temperature and precipitation data, is required. Furthermore, ~~as the~~
235 ~~observational and simulated grids of the two latter variables are typically not available at the same~~
236 ~~horizontal resolution,~~ we seek for a snowfall separation method that accounts for the topographic
237 subgrid-scale variability of snowfall on the ~~the coarser~~ (RCM) grid.

238 **Snowfall bias correction adjustment.** Even the latest generation of RCMs is known to suffer from
239 systematic model biases (e.g., Kotlarski et al., 2014). In GCM-driven setups as employed within the

240 present work these might partly be inherited from the driving GCM. To remove such systematic model
241 biases in temperature and precipitation, a simple bias ~~correction-adjustment~~ methodology ~~is~~ will be
242 developed and employed in the present work. To assess its performance and applicability, different
243 snowfall indices in the bias-~~corrected-adjusted~~ and not bias-~~corrected-adjusted~~ output ~~are~~ will be
244 compared against observation-~~based~~ estimates.

245 **Snowfall projections for the late 21st century.** Climate change signals for various snowfall indices
246 over the Alpine domain and for specific elevation intervals, derived by a comparison of 30-year control
247 and scenario periods, ~~are~~ will be analysed under the assumption of the RCP8.5 emission scenario. In
248 addition, we aim to identify and quantify the main drivers of future snowfall changes and, in order to
249 assess emission scenario uncertainties, compare RCP8.5-based results with experiments assuming
250 the more moderate RCP4.5 emission scenario. Snowfall projections are generally based on three
251 different datasets: (1) raw RCM snowfall where available, (2) RCM snowfall separated from simulated
252 temperature and precipitation, and (3) RCM snowfall separated from simulated temperature and
253 precipitation and additionally bias-adjusted. While all three estimates are compared for the basic
254 snowfall indices in order to assess the robustness of the projections, more detailed analyses are
255 based on dataset (3) only.

256 In addition and as preparatory analysis, we carry out a basic evaluation of RCM-simulated snowfall
257 amounts. This evaluation, however, is subject to considerable uncertainties as a high-quality
258 observation-based reference at the required spatial scale is not available, and the very focus of the
259 present work is laid on the snowfall projection aspect.

260 ~~On centennial time scales, two main drivers of future snowfall changes over the European Alps with~~
261 ~~competing effects on snowfall amounts are apparent: (1) Mean winter precipitation is expected to~~
262 ~~increase over most parts of the European Alps and in most EURO-CORDEX experiments (e.g.,~~
263 ~~Rajczak et al., in prep.; Smiatek et al., 2016) which in principle could lead to higher snowfall amounts.~~
264 ~~(2) Temperatures are projected to considerably rise throughout the annual cycle (e.g., Gobiet et al.,~~
265 ~~2014; Smiatek et al., 2016; Steger et al., 2013) with the general effect of a decreasing snowfall~~
266 ~~frequency and fraction, thus potentially leading to a reduction in overall snowfall amounts changes.~~
267 ~~Separating the above two competing factors is one of the targets of the current study. A potential~~
268 ~~complication is that changes in daily precipitation frequency (here events > 1 mm/day) and~~
269 ~~precipitation intensity (average amount on wet days) can change in a counteracting manner (e.g.,~~
270 ~~Fischer et al., 2015; Rajczak et al., 2013), and that relative changes are not uniform across the event~~
271 ~~category (e.g. Ban et al., 2015; Fischer and Knutti, 2016).~~

272 The article is structured as follows: Section 2 describes the data used and methods employed. In
273 Sections 3 and 4 results of the bias ~~correction-adjustment~~ approach and snowfall projections for the
274 late 21st century are shown, respectively. The latter are further discussed in Section 5 while overall
275 conclusions and a brief outlook are provided in Section 6. Additional supporting figures are provided in
276 the supplementary material (prefix 'S' in Figure numbers).

277 **2 Data and methods**

278 **2.1 Observational data**

279 To estimate observation-based snowfall, two gridded data sets, one for precipitation and one for
280 temperature, derived from station observations and covering the area of Switzerland are used. Both
281 data sets are available on a daily basis with a horizontal resolution of 2 km for the entire evaluation
282 period 1971-2005 (see Sec. 2.3).

283 The gridded precipitation data set (RhiresD) represents a daily analysis based on a high-resolution
284 rain-gauge network (MeteoSwiss, 2013a) consisting of more than 400 stations which has that have a
285 balanced distribution in the horizontal but under-represents high altitudes (Frei and Schär, 1998; Isotta
286 et al., 2014; Konzelmann et al., 2007). Albeit the data set's resolution of 2 km, the effective grid
287 resolution as represented by the mean inter-station distance is about 15 - 20 km and thus comparable
288 to the nominal resolution of the available climate model data (see Sec. 2.2). The dataset has not been
289 corrected for the systematic measurement bias of rain gauges (e.g., Neff, 1977; Sevruk, 1985; Yang et
290 al., 1999).

291 The gridded near-surface air temperature (from now on simply referred to as *temperature*) data set
292 (TabsD) utilises a set of approx. 90 homogeneous long-term station series (MeteoSwiss, 2013b).
293 Despite the high quality of the underlying station series, errors might be introduced by unresolved
294 scales, an uneven spatial distribution and interpolation uncertainty (Frei, 2014). The unresolved effects
295 of land cover or local topography, for instance, probably lead to an underestimation of spatial
296 variability. ~~Another problem arises in inner Alpine valleys, where the presence of cold air pools is~~
297 ~~systematically overestimated. Also note that, while RhiresD provides daily precipitation sums~~
298 ~~aggregated from 6 UTC to 6 UTC of the following day, TabsD is a true daily temperature average from~~
299 ~~midnight UTC to midnight UTC. Due to a high temporal autocorrelation of daily mean temperature this~~
300 ~~slight inconsistency in the reference interval of the daily temperature and precipitation grids is~~
301 ~~expected to not systematically influence our analysis.~~

302 In addition to the gridded temperature and precipitation datasets and in order to validate simulated raw
303 snowfall amounts station-based observations of fresh snow sums (snow depth) at daily resolution from
304 29 stations in Switzerland with data available for at least 80% of the evaluation period 1971-2005 are
305 employed.

306 **2.2 Climate model data**

307 In terms of climate model data we exploit a recent ensemble of regional climate projections made
308 available by EURO-CORDEX (www.euro-cordex.net), the European branch of the World Climate
309 Research Programme's CORDEX initiative (www.cordex.org; Giorgi et al., 2009). RCM simulations for
310 the European domain were run at a resolution of approximately 50 km (EUR-44) and 12.5 km (EUR-
311 11) with both re-analysis boundary forcing (Kotlarski et al., 2014; Vautard et al., 2013) and GCM-
312 forcing (Jacob et al., 2014). ~~We here disregard the reanalysis-driven experiments and employ the. The~~
313 ~~latter include GCM-driven simulations only. These include~~ historical control simulations and future
314 projections based on RCP greenhouse gas and aerosol emission scenarios. Within the present work

315 we employ daily averaged model output of all except two¹GCM-driven EUR-11 simulations for which
316 control, RCP4.5 and RCP8.5 runs are currently were available in December 2016. This yields a total
317 set of 14 GCM-RCM model chains, combining five driving GCMs with seven different RCMs (Tab. 1).
318 We exclusively focus on the higher resolved EUR-11 simulations and disregard the coarser EUR-44
319 ensemble due to the apparent added value of the EUR-11 ensemble with respect to regional-scale
320 climate features in the complex topographic setting of the European Alps (e.g., Giorgi et al., 2016;
321 Torma et al., 2015).

322 It is important to note that each of the sevensix RCMs considered uses an individual grid cell
323 topography field. Model topographies for a given grid cell might therefore considerably differ from each
324 other, and also from the observation-based orography. Hence, it is not meaningful to compare snowfall
325 values at individual grid cells since the latter might be situated at different elevations. Therefore, most
326 analyses of the present work were carried out as a function of elevation, i.e., by averaging climatic
327 features over distinct elevation intervals.

328 **2.3 Analysis domain and periods**

329 The arc-shaped European Alps - with a West-East extent of roughly 1200 km , a total of area 190'000
330 km² and a peak elevation of 4810 m a.s.l. (Mont Blanc) - are the highest and most prominent
331 mountain range which is entirely situated in Europe. In the present work, two different analysis
332 domains are used. The evaluation of the bias correction-adjustment approach depends on the
333 observational data sets RhiresD and TabsD (see Sec. 2.1). As these cover Switzerland only, the
334 evaluation part of the study (Sec. 3) is constrained to the Swiss domain (Fig. 1, bold line). For the
335 analysis of projected changes of different snowfall indices (Sec. 4 and 5) a larger domain covering the
336 entire Alpine crest with its forelands is considered (Fig. 1, coloured region).

337 Our analysis is based on three different time intervals. The evaluation period (EVAL) 1971-2005 iswas
338 used for the calibration and validation of the bias correction-adjustment approach. Future changes of
339 snowfall indices are were computed by comparing a present-day control period (1981-2010, CTRL) to
340 a future scenario period at the end of the 21st century (2070-2099, SCEN). For all periods (EVAL,
341 CTRL and SCEN), the summer months June, July and August (JJA) are excluded from any statistical
342 analysis. In addition to seasonal mean snowfall conditions, i.e., averages over the nine-month period
343 from September to May, we also analyse the seasonal cycle of individual snowfall indices at monthly
344 resolution.

345 **2.4 Analysed snowfall indices and change signals**

346 A set of six different snowfall indices is considered (Tab. 2). Mean snowfall (S_{mean}) refers to the
347 (spatio-) temporally-averaged snowfall amount in mm SWE (note that from this point on we will use the
348 term "mm" as a synonym for "mm SWE" as unit of several snowfall indices). The two indices heavy
349 snowfall (S_{q99}) and maximum 1-day snowfall ($S_{1\text{d}}$) allow the assessment of projected changes in heavy

¹ The HadGEM2-RACMO experiments were excluded due to serious snow accumulation issues over the European Alps. Furthermore, only realization 1 of MPI-M-REMO was included in order to avoid mixing GCM-RCM sampling with pure internal climate variability sampling.

350 snowfall events and amounts. S_{1d} is derived by averaging maximum 1-day snowfall amounts over all
 351 individual months/seasons of a given time period (i.e., by averaging 30 maximum values in the case of
 352 the CTRL and SCEN period), while S_{q99} is calculated from the grid point-based 99th all-day snowfall
 353 percentile of the daily probability density function (PDF) for the entire time period considered. We use
 354 all-day percentiles as the use of wet-day percentiles leads to conditional statements that are often
 355 misleading (see the analysis in Schär et al. 2016). Note that the underlying number of days differs for
 356 seasonal (September-May) and monthly analyses. Snowfall frequency (S_{freq}) and mean snowfall
 357 intensity (S_{int}) are based on a wet-day threshold of 1 mm/day and provide additional information about
 358 the distribution and magnitude of snowfall events, while the snowfall fraction (S_{frac}) describes the ratio
 359 of solid precipitation to total precipitation. As climate models tend to suffer from too high occurrence of
 360 drizzle and as small precipitation amounts are difficult to measure, daily precipitation values smaller or
 361 equal to 0.1 mm were ~~initially~~ set to zero in both the observations and the simulations prior to the
 362 remaining analyses.

363 Projections are assessed by calculating two different types of changes between the CTRL and the
 364 SCEN period. The absolute change signal (Δ) of a particular snowfall index X (see Tab.2)

$$365 \quad \Delta X = X_{SCEN} - X_{CTRL} \quad (1)$$

366 and the relative change signal (δ) which describes the change of the snowfall index as a percentage of
 367 its CTRL period value

$$368 \quad \delta X = \left(\frac{X_{SCEN}}{X_{CTRL}} - 1 \right) \cdot 100 \quad (2)$$

369 To prevent erroneous data interpretation due to possibly ~~ye~~ large relative changes of small CTRL
 370 values, certain grid boxes were masked out before calculating and averaging the signal of change.
 371 This filtering was done by setting threshold values for individual indices and statistics (see Table 2).

372 **2.5 Separating snowfall from total precipitation**

373 Due to (a) the lack of a gridded observational snowfall data set and (b) the fact that not all RCM
 374 simulations available through EURO-CORDEX provide raw snowfall as an output variable, a method
 375 to separate solid from total precipitation depending on near-surface temperature conditions is
 376 developed. ~~This method also allows for a more physically-based bias correction of simulated snowfall~~
 377 ~~amounts (see Sec. 2.6). Due to the temperature dependency of snowfall occurrence, snowfall biases~~
 378 ~~of a given climate model cannot be expected to remain constant under current and future (i.e.,~~
 379 ~~warmer) climate conditions. For instance, a climate model with a given temperature bias might pass~~
 380 ~~the snow-rain temperature threshold earlier or later than reality during the general warming process.~~
 381 ~~Hence, traditional bias correction approaches based only on a comparison of observed and simulated~~
 382 ~~snowfall amounts in the historical climate would possibly fail due to a non-stationary bias structure.~~

383 The simplest approach to separate snowfall from total precipitation is to fractionate the two phases
 384 binary by applying a constant snow fractionation temperature (e.g., de Vries et al., 2014; Schmucki et
 385 al., 2015a; Zubler et al., 2014). More sophisticated methods estimate the snow fraction f_s dependence

386 on air temperature with linear or logistic relations (e.g., Kienzle, 2008; McAfee et al., 2014). In our
 387 case, the different horizontal resolutions of the observational (high resolution of 2 km) and simulated
 388 (coarser resolution of 12 km) data sets further complicate a proper comparison of the respective
 389 snowfall amounts. Thus, we explicitly analysed the snowfall amount dependency on the grid resolution
 390 and exploited possibilities for including subgrid-scale variability in snowfall separation ~~based on coarse~~
 391 ~~grid information~~. This approach is important as especially in Alpine terrain a strong subgrid-scale
 392 variability of near-surface temperatures due to orographic variability has to be expected, with
 393 corresponding effects on the subgrid-scale snowfall fraction.

394 For this preparatory analysis, which is entirely based on observational data, a reference snowfall is
 395 derived. It is based on the approximation of snowfall by application of a fixed temperature threshold to
 396 daily total precipitation amounts on the high resolution observational grid (2 km) and will be termed
 397 *Subgrid method* thereafter: First, the daily snowfall S' at each grid point of the observational data set at
 398 high resolution (2 km) is derived by applying a snow fractionation temperature $T^*=2^\circ\text{C}$. The whole
 399 daily precipitation amount P' is accounted for as snow S' (i.e., $f_s=100\%$) for days with daily mean
 400 temperature $T \leq T^*$. For days with $T > T^*$, S' is set to zero and P' is attributed as rain (i.e., $f_s=0\%$). This
 401 threshold approach with a fractionation temperature of 2°C corresponds to the one applied in previous
 402 works and results appear to be in good agreement with station-based snowfall measurements (e.g.,
 403 Zubler et al., 2014). The coarse grid (12 km) reference snowfall S_{SG} is determined by averaging the
 404 sum of separated daily high resolution S' over all n high-resolution grid points i located within a specific
 405 coarse grid point k . I.e., at each coarse grid point k

$$406 \quad S_{SG} = \frac{1}{n} \cdot \sum_{i=1}^n P'_i [T'_i \leq T^*] = \frac{1}{n} \sum_{i=1}^n S'_i \quad (3)$$

407 For comparison, the same binary fractionation method with a temperature threshold of $T^*=2^\circ\text{C}$ is
 408 directly applied on the coarse 12 km grid (*Binary method*). For this purpose, total precipitation P' and
 409 daily mean temperature T' of the high-resolution data are conservatively remapped to the coarse grid
 410 leading to P and T , respectively. Compared to the *Subgrid method*, the *Binary method* neglects any
 411 subgrid-scale variability of the snowfall fraction. As a result, the *Binary method* underestimates S_{mean}
 412 and overestimates S_{q99} for ~~most~~ elevation intervals (Fig. 2). The underestimation of S_{mean} can be
 413 explained by the fact that even for a coarse grid temperature above T^* individual high-elevation
 414 subgrid cells (at which $T \leq T^*$) can receive substantial snowfall amounts, ~~a process that is not~~
 415 ~~accounted for by the Binary method~~. As positive precipitation-elevation gradients can be assumed for
 416 most parts of the domain (larger total precipitation at high elevations; see e.g. Kotlarski et al., 2012
 417 and Kotlarski et al., 2015 for an Alpine-scale assessment) the neglect of subgrid-scale snowfall
 418 variation in the Binary method hence leads a systematic underestimation of mean snowfall compared
 419 to the Subgrid method. Furthermore, following O'Gorman (2014), heavy snowfall events are expected
 420 to occur in a narrow temperature range below the rain-snow transition. As the *Binary method* in these
 421 temperature ranges always leads to a snowfall fraction of 100%, too large S_{q99} values would result.

422 To take into account these subgrid-scale effects, a more sophisticated approach – referred to as the
 423 *Richards method* – is developed here. This method is based upon a generalised logistic regression
 424 (Richards, 1959). Here, we apply this regression to relate the surface temperature T to the snow

425 fraction f_s by accounting for the topographic subgrid-scale variability. At each coarse grid-point k , the
 426 *Richards method*-based snowfall fraction $f_{s,RI}$ for a given day is hence computed as follows:

$$427 \quad f_{s,RI}(T_k) = \frac{1}{[1 + C_k \cdot e^{D_k \cdot (T_k - T^*)}]^{C_k}} \quad (4)$$

428 with C as the point of inflexion (denoting the point with largest slope), and D the growth rate D
 429 (reflecting the mean slope). T_k is the daily mean temperature of the corresponding coarse grid box k
 430 and $T^*=2^\circ\text{C}$ the snow fractionation temperature. First, we estimate the two parameters C and D of
 431 Equation 4 for each single coarse grid point k by minimizing the least-square distance to the f_s values
 432 derived by the *Subgrid method* via the reference snowfall S_{SG} (local fit). Second, C and D are
 433 expressed as a function of the topographic standard deviation σ_h of the corresponding coarse
 434 resolution grid point only (Fig. S1; global fit). This makes it possible to define empirical functions for
 435 both C and D that can be used for all grid points k in the Alpine domain and that depend on σ_h only.

$$436 \quad \sigma_{h,k} = \sqrt{\frac{\sum_i^n (h_i - \bar{h}_k)^2}{n-1}} \quad (5)$$

$$437 \quad C_k = \frac{1}{(E - \sigma_{h,k} \cdot F)} \quad (6)$$

$$438 \quad D_k = G \cdot \sigma_{h,k}^{-H} \quad (7)$$

439 Through a minimisation of the least square differences the constant parameters in Equations 6 and 7
 440 are calibrated over the domain of Switzerland and using daily data from the period September to May
 441 1971-2005 leading to values of $E=1.148336$, $F=0.000966 \text{ m}^{-1}$, $G=143.84113 \text{ }^\circ\text{C}^{-1}$ and $H=0.8769335$.
 442 Note that σ_h is sensitive to the resolution of the two grids to be compared (cf. Eq. 5). It is a measure for
 443 the uniformity of the underlying topography and has been computed based on the high-resolution
 444 [GTOPO30 digital elevation model \(https://lta.cr.usgs.gov/GTOPO30\)](https://lta.cr.usgs.gov/GTOPO30) aggregated to a regular grid of
 445 [1.25 arc seconds \(about 2 km\) which reflects the spatial resolution of the observed temperature and](#)
 446 [precipitation grids \(cf. Section 2.1\)](#). Small values of σ_h indicate a low subgrid-scale topographic
 447 variability, such as in the Swiss low-lands, while high values result from non-uniform elevation
 448 distributions, such as in areas of inner Alpine valleys. σ_h as derived from GTOPO30 might be different
 449 from the subgrid-scale topographic variance employed by the climate models themselves, which is
 450 however not relevant here as only grid cell-averaged model output is analysed and as we considere σ_h
 451 as a proper estimate of subgrid-scale variability.

452 Figure S1 (panel c) provides an example of the relation between daily mean temperature and daily
 453 snow fraction f_s for grid cells with topographical standard deviations of 50 m and 500 m, respectively.
 454 The snowfall amount S_{RI} for a particular day and a particular coarse grid box is finally obtained by
 455 multiplying the corresponding $f_{s,RI}$ and P values. A comparison with the *Subgrid method* yields very
 456 similar results. For both indices S_{mean} and S_{q99} , mean ratios across all elevation intervals are close to 1
 457 (Fig. 2). At single grid points, maximum deviations are not larger than 1 ± 0.1 . Note that for this
 458 comparison calibration and validation period are identical (EVAL period). Based on this analysis, it has
 459 been decided to separate snowfall according to the *Richards method* throughout this work in both the

460 observations and in the RCMs. The observation-based snowfall estimate obtained by applying the
461 *Richards method* to the observational temperature and precipitation grids after spatial aggregation to
462 the 0.11° RCM resolution will serve as reference for the RCM bias ~~correction~~-adjustment and will be
463 termed *reference* hereafter. One needs to bear in mind that the parameters *C* and *D* of the Richards
464 method were fitted for the Swiss domain only and were later on applied to the entire Alpine domain (cf.
465 Fig. 1).

466 2.6 Bias ~~correction~~-adjustment approach

467 Previous work has revealed partly substantial temperature and precipitation biases of the EURO-
468 CORDEX RCMs over the Alps (e.g. Kotlarski et al., 2014; Smiatek et al., 2016), and one has to expect
469 that the separated snowfall amounts are biased too. This would especially hamper the interpretation of
470 absolute climate change signals of the considered snow indices. We therefore explore possibilities to
471 bias-~~adjust~~correct the simulated snowfall amounts and to directly integrate this bias ~~correction~~
472 adjustment into the snowfall separation framework of Section 2.5. Note that we deliberately employ the
473 term *bias adjustment* as opposed to *bias correction* to make clear that only certain aspects of the
474 snowfall climate are adjusted and that the resulting dataset might be subject to remaining
475 inaccuracies.

476 ~~We compare results with and without employment of the bias correction procedure outlined below.~~ A
477 simple two-step approach that separately accounts for precipitation and temperature biases and their
478 respective influence on snowfall is chosen. The separate consideration of temperature and
479 precipitation biases allows for a more physically-based bias adjustment of snowfall amounts: Due to
480 the temperature dependency of snowfall occurrence, snowfall biases of a given climate model cannot
481 be expected to remain constant under current and future (i.e., warmer) climate conditions. For
482 instance, a climate model with a given temperature bias might pass the snow-rain temperature
483 threshold earlier or later than reality during the general warming process. Hence, traditional bias
484 adjustment approaches based only on a comparison of observed and simulated snowfall amounts in
485 the historical climate would possibly fail due to a non-stationary bias structure. The bias ~~correction~~
486 adjustment is calibrated in the EVAL period for each individual GCM-RCM chain and over the region of
487 Switzerland, and is then applied to both the CTRL and SCEN period of each chain and for the entire
488 Alpine domain. To be consistent in terms of horizontal grid spacing, the observational data sets
489 RhiresD and TabsD (see Sec. 2.1) are conservatively regridded to the RCM resolution beforehand.

490 In a first step, total simulated precipitation was adjusted by introducing an elevation-dependent
491 ~~correction~~-adjustment factor which ~~corrects for~~adjusts precipitation biases regardless of temperature.
492 For this purpose, mean precipitation ratios (RCM simulation divided by observational analysis) for 250
493 m elevation intervals were calculated (Fig. S2). An almost linear relationship of these ratios with
494 elevation was found. Thus, a linear regression between the intervals from 250 m a.s.l. to 2750 m a.s.l.
495 was used for each model chain separately to estimate a robust ~~correction~~-adjustment factor. As the
496 number of both RCM grid points and measurement stations at very high elevations (>2750 m a.s.l.) is
497 small (see Sec. 2.1) and biases are subject to a considerable sampling uncertainty, these elevations
498 were not considered in the regression. Overall the fits are surprisingly precise except for the altitude

499 bins above 2000 m (Fig. S2). The precipitation adjustment factors (P_{AF}) for a given elevation were then
500 obtained as the inverse of the fitted precipitation ratios. Multiplying simulated precipitation P with P_{AF}
501 for the respective model chain and elevation results in the ~~corrected-adjusted~~ precipitation:

$$502 \quad P_{\text{corr-adj}} = P \cdot P_{AF} \quad (8)$$

503 For a given GCM-RCM chain and for each elevation interval, the spatially and temporally averaged
504 corrected total precipitation $P_{\text{corr-adj}}$ approximately corresponds to the observation-based estimate in
505 the EVAL period.

506 In the second step of the bias ~~adjustment~~correction procedure, temperature biases are accounted
507 for. For this purpose the initial snow fractionation temperature $T^*=2^\circ\text{C}$ of the Richards separation
508 method (see Sec 2.5) is shifted to the value T_a^* for which the spatially (Swiss domain) and temporally
509 (September to May) averaged simulated snowfall amounts for elevations below 2750 m a.s.l. match
510 the respective observation-based reference (see above). Compared to the adjustment of total
511 precipitation, T_a^* is chosen independent of elevation, but separately for each GCM-RCM chain, in
512 order to avoid overparameterization and to not over-interpret the elevation dependency of mean
513 snowfall in the snowfall reference grid. After this second step of the bias ~~adjustment~~correction, the
514 spatially ~~(Swiss domain)~~ and temporally ~~(September to May)~~ averaged simulated snowfall amounts
515 below 2750 m a.s.l. by definition match the reference by definition. Hence, the employed simple bias
516 ~~adjustment~~ correction procedure ~~corrects-adjusts~~ domain-mean snowfall biases averaged over the
517 entire season from September to May. It does, however, not correct for biases in the spatial snowfall
518 pattern, in the seasonal cycle, or in the temporal distribution of daily values. Note that, as the
519 underlying high-resolution data sets are available over Switzerland only, the calibration of the bias
520 ~~correction-adjustment~~ methodology is correspondingly restricted, but the ~~correction-adjustment~~ is then
521 applied to the whole Alpine domain. This approach is justified as elevation-dependent mean winter
522 precipitation and temperature biases of the RCMs employed – assessed by comparison against the
523 coarser-resolved EOBS reference dataset (Haylock et al., 2008) - are very similar ~~for over~~ Switzerland
524 and ~~for over~~ the entire Alpine analysis domain (Figs. S3 and S4).

525 **3 Evaluation**

526 **3.1 RCM raw snowfall**

527 We first carry out an illustrative comparison of RCM raw snowfall amounts (for those simulations only
528 that directly provide snowfall flux) against station observations of snowfall, in order to determine
529 whether the simulated RCM snowfall climate contains valid information despite systematic biases. To
530 this end, simulated raw snowfall amounts of nine EURO-CORDEX simulations (see Tab. 1) averaged
531 over 250 m-elevation intervals and over in the range 950 – 1650 m a.s.l. are compared against
532 observations ~~derived from of~~ measured fresh snow sums from 29 MeteoSwiss stations (see Section
533 2.1), with data available for at least 80% of the EVAL period. For this purpose a mean snow density of
534 100 kg/m^3 for the conversion from measured snow height-depth to water equivalent is assumed. Note
535 that this simple validation is subject to considerable uncertainties as it does not explicitly correct for the

536 scale and elevation gap between grid-cell based RCM output and single-site observations. Especially
537 in complex terrain and for exposed sites, point measurements of snow depth might be non-
538 representative for larger-scale conditions (e.g., Grünewald and Lehning, 2015). Also, the conversion
539 from snow depth to snow water equivalent is of approximate nature only, and fresh snow sums might
540 furthermore misrepresent true snowfall in case that snow melt or snow drift occurs between two snow
541 depth readings.

542 At low elevations simulated mean September-May raw snowfall sums match the observations well
543 while differences are larger aloft (Fig. 3a). The positive bias at high elevations might arise from the fact
544 that (the very few) observations were made at ~~a~~ specific locations while simulated grid point values of
545 the corresponding elevation interval might be located in different areas of Switzerland. It might also be
546 explained by positive RCM precipitation and negative RCM temperature biases at high elevations of
547 the Alps (e.g., Kotlarski et al., 2015). At lower elevations, the station network is geographically more
548 balanced and the observations are probably more representative of the respective elevation interval.
549 Despite a clear positive snowfall bias in mid-winter, the RCMs are generally able to reproduce the
550 mean seasonal cycle of snowfall for elevations between 950 m a.s.l. - 1650 m a.s.l. (Fig. 3b). The fact
551 that the major patterns of both the snowfall-elevation relationship and the mean seasonal snowfall
552 cycle are basically well represented indicates the general and physically consistent applicability of
553 RCM output to assess future changes in mean and heavy Alpine snowfall. However, substantial
554 biases in snowfall amounts are apparent and a bias correction adjustment of simulated snowfall
555 seems to be required prior to the analysis of climate change signals of individual snowfall indices.

556 **3.2 Evaluation of the reference snowfall**

557 The snowfall separation employing the Richards method (Section 2.5) and, as a consequence, also
558 the bias adjustment (Section 2.6) make use of the 2 km reference snowfall grid derived by employing
559 the Subgrid method on the observed temperature and precipitation grids. Hence, the final results of
560 this study could to some extent be influenced by inaccuracies and uncertainties of the reference
561 snowfall grid itself. In order to assess the quality of the latter and in absence of a further observation-
562 based reference we here present an approximate evaluation.

563 First, the reference snowfall grid is evaluated against fresh snow sums at the 29 Swiss stations that
564 were also used for evaluating RCM raw snowfall. Note the limitations of such a comparison as outlined
565 in Chapter 3.1. The comparison of black and red markers and lines in Figure 3 indicates a good
566 agreement of mean snowfall at individual elevation intervals (left panel) as well for the mean annual
567 cycle of snowfall at medium elevations (right panel). The reference snowfall grid is obviously a good
568 approximation of site-scale fresh snow sums. Note that similarly to the RCM raw snowfall evaluation,
569 all 2 km reference snowfall grid cells in the respective elevation interval are considered. The good
570 agreement, however, still holds if only those 2 km grid cells covering the 29 site locations are
571 considered (not shown here).

572 Second, both the 2 km reference snowfall grid and the 0.11° reference snowfall grid obtained by
573 employing the Richards method to aggregated temperature and precipitation values (see Section 2.5)
574 are compared against the gridded HISTALP dataset of solid precipitation (Chimani et al., 2011). The

575 latter is provided at a monthly resolution on a 5' grid covering the Greater Alpine Region. It is based on
576 monthly snowfall fraction estimates that are used to scale a gridded dataset of total precipitation. The
577 comparison of the three datasets for the region of Switzerland (for which the 2 km reference snowfall
578 is available) in the EVAL period 1971-2005 yields an approximate agreement of both the magnitude of
579 mean winter snowfall and its spatial pattern. The three data sets differ with respect to their spatial
580 resolution but all show a clear dependency of snowfall on topography and mean September-May
581 snowfall sums above 1000 mm over most parts of the Alpine ridge. Climatologically warm and dry
582 valleys, on the other hand, are represented by minor snowfall amounts of less than 400 m only.

583 As mentioned before these evaluations of the reference snowfall grid are subject to uncertainties and,
584 furthermore, they only cover mean snowfall amounts. However, they provide basic confidence in the
585 applicability of the reference snowfall grid for the purposes of snowfall separation and bias adjustment
586 in the frame of the present study.

587

588 **3.32 Calibration of bias ~~correction~~-adjustment**

589 The analysis of total precipitation ratios (RCM simulations with respect to observations) for the EVAL
590 period, which are computed to carry out the first step of the bias ~~correction~~-adjustment procedure,
591 reveals substantial elevation dependencies. All simulations tend to overestimate total precipitation at
592 high elevations (Fig. S24). This fact might ultimately be connected to an overestimation of surface
593 snow amount in several EURO-CORDEX RCMs as reported by Terzago et al. (2017). As the
594 precipitation ratio between simulations and observations depends approximately linearly ~~depends~~-on
595 elevation, the calculation of P_{AF} via a linear regression of the ratios against elevation (see Sec. 2.6)
596 seems reasonable. By taking the inverse of this linear relation, P_{AF} for every model and elevation can
597 be derived. For the CCLM and RACMO simulations, these correction factors do not vary much with
598 height, while P_{AF} for MPI-ESM - REMO and EC-EARTH - HIRHAM is much larger than 1 in low lying
599 areas, indicating a substantial underestimation of observed precipitation sums (Fig. 4a). However, for
600 most elevations and simulations, P_{AF} is generally smaller than 1, i.e., total precipitation is
601 overestimated by the models. Similar model biases in the winter and spring seasons have already
602 been reported in previous works (e.g., Rajczak et al., in prep.; Smiatek et al., 2016). Especially at high
603 elevations, these apparent positive precipitation biases could be related to observational undercatch,
604 i.e., an underestimation of true precipitation sums by the observational analysis. Frei et al. (2003)
605 estimated seasonal Alpine precipitation undercatch for three elevation intervals. Results show that
606 measurement biases are largest in winter and increase with altitude. However, a potential undercatch
607 (with a maximum of around 40% at high elevations in winter; Frei et al., 2003) can only partly explain
608 the partly substantial overestimation of precipitation found in the present work.

609 After applying P_{AF} to the daily precipitation fields, a snowfall fractionation at the initial T^* of 2 °C (see
610 Eq. (4)) would lead to a snowfall excess in all 14 simulations as models typically experience a cold
611 winter temperature bias. To match the observation-based and spatio-temporally averaged reference
612 snowfall below 2750 m a.s.l., T^* for all models needs to be decreased during the second step of the
613 bias ~~correction~~-adjustment (Fig 4b). The adjusted T_a^* values indicate a clear positive relation with the

614 mean temperature bias in the EVAL period. This feature is expected since the stronger a particular
615 model's cold bias the stronger the required adjustment of the snow fractionation temperature T^*
616 towards lower values in order to avoid a positive snowfall bias. Various reasons for the scatter around
617 a simple linear relation in Figure 4b can be thought of. These include remaining spatial inaccuracies of
618 the corrected precipitation grid, elevation-dependent temperature biases and misrepresented
619 temperature-precipitation relationships at daily scale. Note that precipitation and temperature biases
620 heavily depend on the GCM-RCM chain and seem to be rather independent from each other. While
621 EC-EARTH – RACMO, for instance, shows one of the best performances in terms of total
622 precipitation, its temperature bias of close to -5 °C is the largest deviation in our set of simulations.
623 Concerning the partly substantial temperature biases of the EURO-CORDEX models shown in Figure
624 4 b, their magnitude largely agrees with Kotlarski et al. (2014; in reanalysis-driven simulations) and
625 Smiatek et al. (2016).

626 **3.43 Evaluation of snowfall indices**

627 We next assess the performance of the bias correction-adjustment procedure by comparing snowfall
628 indices derived from separated and bias-corrected-adjusted RCM snowfall amounts against the
629 observation-based reference. The period for which this comparison is carried out is EVAL, i.e., it is
630 identical to the calibration period of the bias correction-adjustment. We hence do not intend a classical
631 cross validation exercise with separate calibration and validation periods, but try to answer the
632 following two questions: (a) Which aspects of the Alpine snowfall climate are corrected-foradjusted,
633 and (b) for which aspects do biases remain even after application of the bias correction-adjustment
634 procedure.

635 Figure 5 shows the evaluation results of the six snowfall indices based on the separated and not bias-
636 corrected-adjusted simulated snowfall ($RCM_{sep+nb_{ae}}$), and the separated and bias-corrected-adjusted
637 simulated snowfall ($RCM_{sep+b_{ae}}$). In the first case the snowfall separation of raw precipitation is
638 performed with $T^*=2^{\circ}C$, while in the second case precipitation is corrected-adjusted and the separation
639 is performed with a bias-adjusted temperature T^*_a . The first column represents the mean September
640 to May statistics, while columns 2-4 depict the seasonal cycle at monthly resolution for three distinct
641 elevation intervals.

642 The analysis of S_{mean} confirms that $RCM_{sep+b_{ae}}$ is able to reproduce the observation-based reference in
643 the domain mean as well as in most individual elevation intervals. The domain-mean agreement is a
644 direct consequence of the design of the bias correction-adjustment procedure (see above).
645 $RCM_{sep+nb_{ae}}$, on the other hand, consistently overestimates S_{mean} by up to a factor of 2.5 as a
646 consequence of positive precipitation and negative temperature biases (cf. Fig. 4). Also the seasonal
647 cycle of S_{mean} for $RCM_{sep+b_{ae}}$ yields a satisfying performance across all three elevation intervals, while
648 $RCM_{sep+nb_{ae}}$ tends to produce too much snowfall over all months and reveals an increasing model
649 spread with elevation.

650 For the full domain and elevations around 1000 m, the observation-based reference indicates a mean
651 S_{freq} of 20% between September and May. Up to 1000 m a.s.l. $RCM_{sep+b_{ae}}$ reflects the increase of this

652 index with elevation adequately. However, towards higher elevations the approximately constant S_{freq}
653 of 30% in the reference is not captured by the simulation-derived snowfall. Notably during wintertime,
654 both $\text{RCM}_{\text{sep+b}_{\text{ae}}}$ and $\text{RCM}_{\text{sep+nb}_{\text{ae}}}$ produce too many snowfall days, i.e., overestimate snowfall
655 frequency. This feature is related to the fact that climate models typically tend to overestimate the wet
656 day frequency over the Alps especially in wintertime (Rajczak et al., 2013) and that the bias ~~correction~~
657 adjustment procedure employed does not explicitly correct for potential biases in precipitation
658 frequency. Due to the link between mean snowfall on one side and snowfall frequency and mean
659 intensity on the other side, opposite results are obtained for the mean snowfall intensity S_{int} .
660 $\text{RCM}_{\text{sep+b}_{\text{ae}}}$ largely underestimates mean intensities during snowfall days while $\text{RCM}_{\text{sep+nb}_{\text{ae}}}$ typically
661 better reflects the reference. Nevertheless, deviations during winter months at mid-elevations are not
662 negligible. Mean September-May S_{frac} in the reference exponentially increases with elevation. This
663 behaviour is reproduced by both $\text{RCM}_{\text{sep+b}_{\text{ae}}}$ and $\text{RCM}_{\text{sep+nb}_{\text{ae}}}$. Notwithstanding, $\text{RCM}_{\text{sep+b}_{\text{ae}}}$ results are
664 more accurate compared to $\text{RCM}_{\text{sep+nb}_{\text{ae}}}$, which turns out to be biased towards too large snowfall
665 fractions.

666 For the two heavy snowfall indices S_{q99} and $S_{1\text{d}}$, $\text{RCM}_{\text{sep+nb}_{\text{ae}}}$ appears to typically match the reference
667 better than $\text{RCM}_{\text{sep+b}_{\text{ae}}}$. Especially at high elevations, $\text{RCM}_{\text{sep+b}_{\text{ae}}}$ produces too low snowfall amounts.
668 This again ~~highlights-illustrates~~ the fact that the bias ~~adjustment correction~~ procedure is designed to
669 ~~correct-adjust for~~ biases in mean snowfall, but does not necessarily improve further aspects of the
670 simulated snowfall climate.

671 The spatial patterns of S_{mean} for the 14 $\text{RCM}_{\text{sep+b}_{\text{ae}}}$ simulations from September to May are presented
672 in Figure 6. The observational-based reference (lower right panel) reveals a snowfall distribution with
673 highest values along the Alpine main ridge, whereas the Swiss plateau, Southern Ticino and main
674 valleys such as the Rhône and Rhine valley experience less snowfall. Almost all bias-~~corrected~~
675 adjusted models are able to represent the overall picture with snow-poor lowlands and snow-rich
676 Alpine regions. Nevertheless substantial differences to the observations concerning the spatial
677 snowfall pattern can arise. EC-EARTH - HIRHAM, for example, is subject to a "pixelated" structure.
678 This could be the result of frequent grid-cell storms connected to parameterisations struggling with
679 complex topographies. Such inaccuracies in the spatial pattern are not corrected for by our simple bias
680 ~~correction-adjustment~~ approach ~~which that~~ only targets domain-mean snowfall amounts at elevations
681 below 2750 m a.s.l. and that does not considerably modify the simulated spatial snowfall patterns..
682 Note that these patterns are obviously strongly determined by the RCM itself and only slightly depend
683 on the driving GCM (see, for instance, the good agreement among the CCLM and the RCA
684 simulations).

685 In summary, after applying the bias ~~adjustment correction~~ to the simulations most snowfall indices are
686 fairly well represented at elevations below 1000 m a.s.l.. With increasing altitude and smaller sample
687 sizes in terms of number of grid cells, reference and $\text{RCM}_{\text{sep+b}_{\text{ae}}}$ diverge. This might be caused by the
688 remaining simulated overestimation of S_{freq} and an underestimation of S_{int} . While the bias adjustment
689 ~~correction~~ approach leads to a reduction of S_{int} due to the total precipitation adjustment, S_{freq} is only
690 slightly modified by this correction and by the adjustment of T^* . Nevertheless, these two parameters

691 strongly influence other snowfall indices. The counteracting effects of overestimated S_{freq} and
692 underestimated S_{int} result in appropriate amounts of S_{mean} whereas discrepancies for S_{q99} and S_{1d} are
693 mainly driven by the underestimation of S_{int} .

694 **4 Snowfall projections for the late 21st century**

695 For the study of climate change signals, the analysis domain is extended to the entire Alps (see Sec.
696 2.3). Due to the identified difficulties of bias-~~correcting-adjusting~~ certain snowfall indices (see Sec
697 3.43), emphasis is laid upon relative signals of change (see Eq. 2). This type of change can be
698 expected to be less dependent on the remaining inaccuracies after the ~~correctionadjustment~~. If not
699 stated otherwise, all results in this Section are based on the RCM_{sep+base} data, i.e., on separated and
700 bias-~~corrected-adjusted~~ RCM snowfall, and on the RCP8.5 emission scenario.

701 Projections for seasonal S_{mean} show a considerable decrease over the entire Alpine domain (Fig. 7).
702 Most RCMs project largest percentage losses of more than 80% across the Alpine forelands ~~and~~
703 ~~especially in its topographic depressions~~ such as the Po ~~and Rhone v~~Valleys ~~or Western France~~. Over
704 the Alpine ridge, reductions are smaller but still mostly negative. Elevated regions between
705 Southeastern Switzerland, Northern Italy and Austria seem to be least affected by the overall snowfall
706 reduction. Some of the simulations (e.g., CNRM-RCA, MPI-ESM-RCA or MPI-ESM-REMO) project
707 only minor changes in these regions. Experiments employing the same RCM but different driving
708 GCMs (e.g. the four simulations of RCA), but also experiments employing the same GCM but different
709 RCMs (e.g. the four simulations driven by EC-EARTH, ~~though different realizations~~) can significantly
710 disagree in regional-scale change patterns and especially in the general magnitude of change. This
711 highlights a strong influence of both the driving GCMs and the RCMs themselves on snowfall changes,
712 representing effects of ~~large-scale~~ circulation and meso-scale response, respectively.

713 A more detailed analysis is provided in Fig. 8 ~~that-which~~ addresses the vertical and seasonal
714 distribution of snowfall changes. It reveals that relative (seasonal mean) changes of S_{mean} appear to be
715 strongly dependent on elevation (Fig.8, top left panel). The multi-~~model~~ mean change ranges from -
716 80% at low elevations to -10% above 3000 m a.s.l.. Largest differences between neighbouring
717 elevation intervals are obtained from 750 m a.s.l. to 1500 m a.s.l.. Over the entire Alps, the results
718 show a reduction of S_{mean} by -35% to -55% with a multi-~~model~~ mean of -45%. The multi-~~model~~ spread
719 appears to be rather independent of elevation and is comparably small, confirming that, overall, the
720 spatial distributions of the change patterns are similar across all model chains (cf. Fig. 7). All
721 simulations point to decreases over the entire nine-month period September to May for the two
722 elevation intervals <1000 m a.s.l. and 1000 to 2000 m a.s.l.. Above 2000 m a.s.l., individual
723 simulations show an increase of S_{mean} by up to 20% in mid-winter which ~~forces-the-leads to a slightly~~
724 ~~positive change in~~ multi-~~model~~ mean ~~change-to-be-slightly-positive~~ in January and February.

725 Decreases of S_{freq} are very similar to change-s_{in} mean snowfall. Mean September-May changes are
726 largest below 1000 m a.s.l., while differences among elevation intervals become smaller ~~in-the-upper~~
727 ~~partat higher elevations~~. In-between is a transition zone with rather strong changes with elevation,
728 ~~which approximately corresponds to the mean elevation of the September-May zero-degree line in~~

729 | [today's climate \(e.g., Ceppi et al., 2012; MeteoSchweiz, 2016\)](#). Individual simulations with large
730 reductions in S_{mean} , such as the RCA experiments, also project strongest declines in S_{freq} . In contrast,
731 the mean snowfall intensity S_{int} is subject to smallest percentage variations in our set of snowfall
732 indices. Strong percentage changes for some models in September are due to the small sample size
733 (only few grid points considered) and the low snowfall amounts in this month. Apart from mid
734 elevations with decreases of roughly -10%, mean intensities from September to May are projected to
735 remain almost unchanged by the end of the century. For both seasonal and monthly changes, model
736 | agreement is best for high elevations while the multi-model spread is largest for lowlands. Large model
737 spread at low elevations might be caused by the small number of grid points used for averaging over
738 the respective elevation interval, especially in autumn and spring.

739 Similar results are obtained for the heavy snowfall indices S_{q99} and S_{1d} . While percentage decreases
740 at lowermost elevations are even larger than for S_{mean} , losses at high elevations are less pronounced,
741 resulting in similar domain-mean change signals for heavy and mean snowfall. Substantial differences
742 between monthly δS_{q99} and δS_{1d} appear at elevations below 1000 m a.s.l.. Here, percentage losses of
743 S_{q99} are typically slightly more pronounced. Above 2000 m a.s.l. both indices appear to remain almost
744 | constant between January and March with change signals close to zero. The multi-model mean
745 changes even hint to slight increases of both indices. Concerning changes in the snowfall fraction, i.e.,
746 in the relative contribution of snowfall to total precipitation, our results indicate that current seasonal
747 and domain mean S_{frac} might drop by about -50% (Fig. 8, lowermost row). Below 1000 m a.s.l., the
748 | strength of the signal is almost independent of the month, and multi-model average changes of the
749 snow fraction of about -80% are obtained. At higher elevations changes during mid-winter are less
750 pronounced compared to autumn and spring but still negative.

751 **5 Discussion**

752 **5.1 Effect of temperature, snowfall frequency and intensity on snowfall changes**

753 The results in Section 4 indicate substantial changes of snowfall indices over the Alps in regional
754 climate projections. With complementary analyses presented in Figures 9 and 10 we shed more light
755 on the responsible mechanisms, especially concerning projected changes in mean and heavy
756 snowfall. For this purpose Figures 9a-b,e-f show the relationship of both mean and heavy snowfall
757 amounts in the CTRL period and their respective percentage changes with the climatological CTRL
758 temperature of the respective (climatological) month, elevation interval and GCM-RCM chain. For
759 absolute amounts (S_{mean} , S_{q99} ; Fig. 9a,e) a clear negative relation is found, i.e., the higher the CTRL
760 temperature the lower the snowfall amounts. For S_{mean} the relation levels off at mean temperatures
761 higher than about 6°C with mean snowfall amounts close to zero. For temperatures below about -6°C
762 a considerable spread in snowfall amounts is obtained, i.e., mean temperature does not seem to be
763 the controlling factor here. Relative changes of both quantities (Fig. 9b,f), however, are strongly
764 controlled by the CTRL period's temperature level with losses close to 100% for warm climatic settings
765 and partly increasing snowfall amounts for colder climates. This dependency of relative snowfall
766 changes on CTRL temperature is in line with previous works addressing future snowfall changes on

767 both hemispheric and regional scales (de Vries et al., 2014; Krasting et al., 2013; Räisänen, 2016).
768 The spread of changes within a given CTRL temperature bin can presumably be explained by the
769 respective warming magnitudes that differ between elevations, months and GCM-RCM chains. About
770 half of this spread can be attributed to the month and the elevation alone (compare the spread of the
771 | black markers to the one of the red markers which indicate multi-model averages).

772 For most months and elevation intervals, percentage reductions in S_{mean} and S_{q99} reveal an almost
773 linear relationship with δS_{freq} (Fig. 9c, g). The decrease of S_{freq} with future warming can be explained
774 by a shift of the temperature probability distribution towards higher temperatures, leading to fewer
775 days below the freezing level (Fig. 10, top row). Across the three elevation intervals <1000 m a.s.l.,
776 | 1000-2000 m a.s.l. and > 2000 m a.s.l., relative changes in the number of days with temperatures
777 below the freezing level ($T \leq 0^\circ\text{C}$) are in the order of -65%, -40% and -20%, respectively (not shown).
778 This approximately corresponds to the simulated decrease of S_{freq} (cf. Fig 8), which in turn, is of a
779 similar magnitude as found in previous works addressing future snowfall changes in the Alps
780 (Schmucki et al., 2015b; Zubler et al., 2014). Due to the general shift of the temperature distribution
781 and the “loss” of very cold days (Fig. 10, top row) future snowfall furthermore occurs in a narrower
782 temperature range (Fig. 10, second row).

783 Contrasting this general pattern of frequency-driven decreases of both mean and heavy snowfall, no
784 changes or even slight increases of S_{mean} , S_{q99} and S_{1d} at high elevations are expected in mid-winter
785 (see Fig. 8). This can to some part be explained by the general increase of total winter precipitation
786 (Rajczak et al., in prep; Smiatek et al., 2016) that obviously offsets the warming effect in high-elevation
787 regions where a substantial fraction of the future temperature PDF is still located below the rain-snow
788 transition (Fig. 10, top row). This process has also been identified in previous works to be, at last
789 partly, responsible for future snowfall increases (de Vries et al., 2014; Krasting et al., 2013; Räisänen,
790 2016). Furthermore, the magnitude of the increases of both mean and heavy snowfall is obviously
791 driven by positive changes of S_{int} , while S_{freq} remains constant (Fig. 9c,g). An almost linear relationship
792 between positive changes of S_{int} and positive changes of S_{mean} and S_{q99} is obtained (Fig. 9d,h; upper
793 right quadrants). Nevertheless, the high-elevation mid-winter growth in S_{mean} is smaller than the
794 identified increases of mean winter total precipitation. This can be explained by the persistent
795 decrease of S_{frac} during the cold season (see Fig. 8, lowermost row).

796 For elevation intervals with simulated monthly temperatures between -6°C and 0°C in the CTRL
797 period, S_{mean} appears to decrease stronger than S_{q99} (cf. Fig. 9b,f). O’Gorman (2014) found a very
798 similar behaviour when analysing mean and extreme snowfall projections over the Northern
799 Hemisphere within a set of GCMs. This finding is related to the fact that future snowfall decreases are
800 mainly governed by a decrease of snowfall frequency while snowfall increases in high-elevated
801 regions in mid-winter seem to be caused by increases of snowfall intensity. It can obviously be
802 explained by the insensitivity of the temperature interval at which extreme snowfall occurs to climate
803 warming and by the shape of the temperature – snowfall intensity distribution itself (Fig. 10, third row).
804 The likely reason behind positive changes of S_{int} at high-elevated and cold regions is the higher water
805 holding capacity of the atmosphere in a warmer climate. According to the Clausius-Clapeyron relation,

806 saturation vapour pressure increases by about 7% per degree warming (Held and Soden, 2006).
807 Previous studies have shown that simulated changes of heavy and extreme precipitation (though not
808 necessarily targeting the daily temporal scale and moderate extremes as in our case) are consistent
809 with this theory (e.g., Allen and Ingram, 2002; Ban et al., 2015). In terms of snowfall, we find the
810 Clausius-Clapeyron relation to be applicable for negative temperatures up to approximately -5°C as
811 well (Fig. 10, third row, dashed lines). Inconsistencies for temperatures between -5°C and 0°C are due
812 to a snow fraction $sf < 100\%$ for corresponding precipitation events.

813 For further clarification, Figure 11 schematically illustrates the governing processes behind the
814 changes of mean and heavy snowfall that differ between climatologically warm (decreasing snowfall)
815 and climatologically cold climates (increasing snowfall). As shown in Figure 10 (third row), the mean
816 S_{int} distribution is rather independent on future warming and similar temperatures are associated with
817 similar mean snowfall intensities. In particular, heaviest snowfall is expected to occur slightly below the
818 freezing level in both the CTRL and the SCEN period (Fig. 11a). How often do such conditions prevail
819 in the two periods? In a warm current climate, i.e., at low elevations or in the transition seasons, heavy
820 snowfall only rarely occurs as the temperature interval for highest snowfall intensity is already situated
821 in the left tail of the CTRL period's temperature distribution (Fig. 11b). With future warming, i.e., with a
822 shift of the temperature distribution to the right, the probability for days to occur in the heavy snowfall
823 temperature interval (dark grey shading) decreases stronger than the probability of days to occur in
824 the overall snowfall regime (light grey shading). This results in (1) a general decrease of snowfall
825 frequency, (2) a general decrease of mean snowfall intensity and (3) a general and similar decrease of
826 both mean and heavy snowfall amounts. In contrast, at cold and high-elevated sites CTRL period
827 temperatures are often too low to trigger heavy snowfall since a substantial fraction of the temperature
828 PDF is located to the left of the heavy snowfall temperature interval (Fig. 11 c). The shifted distribution
829 in a warmer SCEN climate, however, peaks within the temperature interval that favours heavy
830 snowfall. This leads to a probability increase for days to occur in the heavy snowfall temperature range
831 despite the general reduction in S_{req} (lower overall probability of days to occur in the entire snowfall
832 regime, light grey). As a consequence, mean S_{int} tends to increase and the reduction of heavy
833 snowfall amounts is less pronounced (or even of opposing sign) than the reduction in mean snowfall.
834 For individual (climatologically cold) regions and seasons, the increase of mean S_{int} might even
835 compensate the S_{req} decrease, resulting in an increase of both mean and heavy snowfall amounts.
836 Note that in a strict sense these explanations only hold in the case that the probability of snowfall to
837 occur at a given temperature does not change considerably between the CTRL and the SCEN period.
838 This behaviour is approximately given-found (Fig. 10, bottom row), which presumably indicates only
839 minor contributions of large scale circulation changes and associated humidity changes on both the
840 temperature - snowfall frequency and the temperature - snowfall intensity relation.

841 5.2 Emission scenario uncertainty

842 The projections presented in the previous sections are based on the RCP8.5 emission scenario, but
843 will depend on the specific emission-scenario considered. To assess this type of uncertainty we here
844 compare the RCM_{sep+bae} simulations for the previously shown RCP8.5 emission scenario against those
845 assuming the more moderate RCP4.5 scenario. As a general picture, the weaker RCP4.5 scenario is

846 associated with less pronounced changes of snowfall indices (Fig. 12). Differences in mean seasonal
847 δS_{mean} between the two emission scenarios are most pronounced below 1000 m a.s.l. where
848 percentage changes for RCP4.5 are about one third smaller than for RCP8.5. At higher elevations,
849 multi-model mean changes better agree and the multi-model ranges for the two emission scenarios
850 start overlapping, i.e., individual RCP4.5 experiments can be located in the RCP8.5 multi-model range
851 and vice versa. Over the entire Alpine domain, about -25% of current snowfall is expected to be lost
852 under the moderate RCP4.5 emission scenario while a reduction of approximately -45% is projected
853 for RCP8.5. For seasonal cycles, the difference of δS_{mean} between RCP4.5 and RCP8.5 is similar for
854 most months and slightly decreases with altitude. Above 2000 m a.s.l., the simulated increase of S_{mean}
855 appears to be independent of the chosen RCP in January and February, while negative changes
856 before and after mid-winter are more pronounced for RCP8.5. Alpine domain mean δS_{q99} almost
857 doubles under the assumption of stronger GHG emissions. This is mainly due to differences at low
858 elevations whereas above 2000 m a.s.l. δS_{q99} does not seem to be strongly affected by the choice of
859 the emission scenario. Differences in monthly mean changes are in close analogy to δS_{mean} . Higher
860 emissions lead to a further negative shift in δS_{q99} . Up to mid-elevations differences are rather
861 independent of the season. However, at highest elevations and from January to March, differences
862 between RCP4.5 and RCP8.5 are very small.

863 Despite the close agreement of mid-winter snowfall increases at high elevations between the two
864 emission scenarios, obvious differences in the spatial extent of the region of mean seasonal snowfall
865 increases can be found (cf Figs. S65 and 7 for δS_{mean} , and Figs. S76 and S87 for δS_{q99}). In most
866 simulations, the number of grid cells along the main Alpine ridge that show either little change or even
867 increases of seasonal mean S_{mean} or S_{q99} is larger for RCP4.5 than for RCP8.5 with its larger warming
868 magnitude.

869 5.3 Intercomparison of projections with separated and raw snowfall

870 The snowfall projections presented above are based on the RCM_{sep+ba} data set, i.e. on separated and
871 bias-adjusted snowfall amounts. To assess the robustness of these estimates we here compare the
872 obtained change signals against the respective signals based on ~~An intercomparison of relative~~
873 ~~change signals for RCM_{sep+bc} (separated and bias-corrected), RCM_{sep+nbae} (separated and not bias-~~
874 ~~corrected/adjusted) and simulated raw snowfall output (RCM_{raw}).~~ based on ~~This comparison is~~
875 restricted to the nine RCMs providing raw snowfall as output variable (see Tab. 1).

876 The three different change estimates agree well with each other In terms of relative snowfall change
877 signals reveals no substantial differences (Fig. 13, top row). ~~In the three data sets, m~~Multi-model mean
878 relative changes are very similar for all analysed snowfall indices and elevation intervals. In many
879 cases, separated and not bias-adjusted snowfall (RCM_{sep+nba}) is subject to slightly smaller percentage
880 decreases. Furthermore, mMulti-model mean differences between RCM_{sep+bae}, RCM_{sep+nbae} and
881 RCM_{raw} simulations are smaller than the corresponding multi-model spread of RCM_{sep+bae} simulations
882 and emission scenario uncertainties (cf. Figs. 12, 13 and S108).

883 | This ~~agreement in terms of relative change signals finding~~ is in contrast to absolute change
884 | characteristics (Fig. 13, bottom row). Results based on the three data sets agree in the sign of change,
885 | but not in their magnitude, especially at high elevations >2000 m a.s.l.. As the relative changes are
886 | almost identical, the absolute changes strongly depend upon the treatment of biases in the control
887 | climate.

888 | -In summary, these findings indicate that (a) the snowfall separation method developed in the present
889 | work yields rather good proxies for relative changes of snowfall indices in raw RCM output (which is
890 | ~~not available for all for many~~ GCM-RCM chains ~~not available~~), and that (b) the additional bias ~~-~~
891 | ~~adjustment correction~~ of separated snowfall amounts only has a weak influence on relative change
892 | signals of snowfall indices, but can have substantial effects on absolute changes.

893 | **6 Conclusions and outlook**

894 | The present work makes use of state-of-the-art EURO-CORDEX RCM simulations to assess changes
895 | of snowfall indices over the European Alps by the end of the 21st century. For this purpose, snowfall is
896 | separated from total precipitation using near-surface air temperature in both the RCMs and in the an
897 | ~~observation-based estimates~~ on a daily basis. The analysis yields a number of robust signals,
898 | consistent across a range of climate model chains and across emission scenarios. Relating to the
899 | main objectives we find the following:

900 | **Snowfall separation on an RCM grid.** Binary snow fractionation with a fixed temperature threshold
901 | on coarse-resolution grids (with 11 km resolution) leads to an underestimation of mean snowfall and
902 | an overestimation of heavy snowfall. To overcome these deficiencies, the Richards snow fractionation
903 | method is implemented. This approach expresses that the coarse-grid snow fraction depends not only
904 | on daily mean temperature, but also on topographical subgrid-scale variations. Accounting for the
905 | latter results in better estimates for mean and heavy snowfall. However, due to limited observational
906 | coverage the parameters of this method are fitted for Switzerland only and are then applied to the
907 | entire Alpine domain. Whether this spatial transfer is robust could further be investigated by using
908 | observational data sets covering the full domain of interest but is out of the scope of this study.

909 | **Snowfall bias ~~correction~~ adjustment.** Simulations of the current EURO-CORDEX ensemble are
910 | subject to considerable biases in precipitation and temperature, which translate into biased snowfall
911 | amounts. In the EVAL period, simulated precipitation is largely overestimated, with increasing biases
912 | toward higher altitudes. On the other hand, simulated near surface temperatures are generally too low
913 | with largest deviations over mountainous regions. These findings were already reported in previous
914 | studies for both the current EURO-CORDEX data set but also for previous RCM ensembles (e.g. Frei
915 | et al., 2003; Kotlarski et al., 2012; Kotlarski et al., 2015; Rajczak et al., 2013; Smiatek et al., 2016). By
916 | implementing a simple bias ~~adjustment~~ ~~correction~~ approach, we are able to partly reduce these biases
917 | and the associated model spread, which should enable more robust change estimates. The ~~corrected~~
918 | adjusted model results reproduce the seasonal cycles of mean snowfall fairly well. However,
919 | substantial biases remain in terms of heavy snowfall, snowfall intensities (which in general are
920 | overestimated), snowfall frequencies, and spatial snowfall distributions. Further improvements might

921 | be feasible by using more sophisticated bias ~~adjustment correction~~ methods, such as quantile
922 | mapping (e.g., Rajczak et al., 2016), local intensity scaling of precipitation (e.g., Schmidli et al., 2006),
923 | or weather generators (e.g. Keller et al., 2016). Advantages of the approach employed here are its
924 | simplicity, its direct linkage to the snowfall separation method and, as a consequence, its potential
925 | ability to account for non-stationary snowfall biases. Furthermore, a comparison to simulated raw
926 | snowfall for a subset of nine simulations revealed that relative change signals are almost independent
927 | of the chosen post-processing strategy.

928 | **Snowfall projections for the late 21st century.** Snowfall climate change signals are assessed by
929 | deriving the changes in snowfall indices between the CTRL period 1981 - 2010 and the SCEN period
930 | 2070 - 2099. Our results show that by the end of the 21st century, snowfall over the Alps will be
931 | considerably reduced. Between September and May mean snowfall is expected to decrease by
932 | approximately -45% (multi-model mean) under an RCP8.5 emission scenario. For the more moderate
933 | RCP4.5 scenario, multi-model mean projections show a decline of -25%. These results are in good
934 | agreement with previous works (e.g. de Vries et al., 2014; Piazza et al., 2014, Räisänen, 2016). Low-
935 | lying areas experience the largest percentage changes of more than -80%, while the highest Alpine
936 | regions are only weakly affected. Variations of heavy snowfall, defined by the 99% all-day snowfall
937 | percentile, show ~~at low-lying elevations~~ an even more pronounced signal at low-lying elevations. With
938 | increasing elevation, percentage changes of heavy snowfall are generally smaller than for mean
939 | snowfall. O'Gorman (2014) found a very similar behaviour by analysing projected changes in mean
940 | and extreme snowfall over the entire Northern Hemisphere. He pointed out that heavy and extreme
941 | snowfall occurs near an optimal temperature (near or below freezing, but not too cold), which seems to
942 | be independent of climate warming. We here confirm this ~~conclusion finding~~. At mid and high
943 | elevations ~~the optimal temperature for~~ heavy snowfall in a warmer climate will still occur in ~~a warmer~~
944 | ~~climate the optimal temperature range~~ and, hence, heavy snowfall amounts will decrease less strongly
945 | compared to mean snowfall, and may even increase in some areas.:-

946 | At first approximation, the magnitude of future warming strongly influences the reduction of mean and
947 | heavy snowfall by modifying the snowfall frequency. Snowfall increases may however occur at high
948 | (and thus cold) elevations, and these are not caused by frequency changes. Here, snowfall increases
949 | due to (a) a general increase of total winter precipitation combined with only minor changes in snowfall
950 | frequency, and (b) more intense snowfall. This effect has a pronounced altitudinal distribution and may
951 | be particularly strong under conditions (depending upon location and season) where the current
952 | climate is well below freezing. Such conditions may experience a shift towards a ~~more snowfall-~~
953 | ~~friendly~~ temperature range more favourable to snowfall (near or below freezing, but not too cold) with
954 | corresponding increases of mean snowfall, despite a general decrease of the snowfall fraction.

955 | The identified future changes of snowfall over the Alps can lead to a variety of impacts in different
956 | sectors. With decreasing snowfall frequencies and the general increase of the snowline (e.g.,
957 | Beniston, 2003; Gobiet et al., 2014; Hantel et al., 2012), both associated with temperature changes,
958 | ski lift operators are looking into an uncertain future. A shorter snowfall season will likely put them
959 | under greater financial pressure. Climate change effects might be manageable only for ski areas

960 reaching up to high elevations (e.g. Elsasser and Bürki, 2002). Even so these resorts might start later
961 into the ski season, the snow conditions into early spring could change less dramatically due to
962 projected high-elevation snowfall increases in mid-winter. A positive aspect of the projected decrease
963 in snowfall frequency might be a reduced expenditures for airport and road safety (e.g., Zubler et al.,
964 2015).

965 At lower altitudes, an intensification of winter precipitation, combined with smaller snowfall fractions
966 (Serquet et al., 2013), increases the flood potential (Beniston, 2012). Snow can act as a buffer by
967 releasing melt water constantly over a longer period of time. With climate warming, this storage
968 capacity is lost, and heavy precipitation immediately drains into streams and rivers which might not be
969 able to take up the vast amount of water fast enough. Less snowmelt will also have impacts on
970 hydropower generation and water management (e.g., Weingartner et al., 2013). So far, many Alpine
971 regions are able to bypass dry periods by tapping melt water from mountainous regions. With reduced
972 snow-packs due to less snowfall, water shortage might become a serious problem in some areas.

973 Regarding specific socio-economic impacts caused by extreme snowfall events, conclusions based on
974 the results presented in this study are difficult to draw. It might be possible that the 99% all-day
975 snowfall percentile we used for defining heavy snowfalls, is not appropriate to speculate about future
976 evolutions of (very) rare events (Schär et al., 2016). To do so, one might consider applying a
977 generalized extreme value (GEV) analysis which is more suitable for answering questions related to
978 rare extreme events.

979 **7 Data Availability**

980 The EURO-CORDEX RCM data analysed in the present work are publicly available - parts of
981 them for non-commercial use only - via the Earth System Grid Federation archive (ESGF;
982 e.g., <https://esgf-data.dkrz.de>). The observational datasets RHiresD and TabsD as well as
983 the snow depth data for Switzerland are available for research and educational purposes
984 from kundendienst@meteoschweiz.ch. The analysis code is available from the
985 corresponding author on request.

986 **8 Competing Interests**

987 The authors declare that they have no conflict of interest.

988 **9 Acknowledgements**

989 We gratefully acknowledge the support of Jan Rajczak, Urs Beyerle and Curdin Spirig (ETH Zurich) as
990 well as Elias Zubler (MeteoSwiss) in data acquisition and pre-processing. Christoph Frei (MeteoSwiss)
991 and Christoph Marty (WSL-SLF) provided important input on specific aspects of the analysis. [The](#)
992 [GTOPO30 digital elevation model is available from the U.S. Geological Survey.](#) Finally, we thank the

993 climate modelling groups of the EURO-CORDEX initiative for producing and making available their
994 model output.

995 **10 References**

- 996 Abegg, B. A., S., Crick, F., and de Montfalcon, A.: Climate change impacts and adaptation in winter tourism, in:
997 Climate change in the European Alps: adapting winter tourism and natural hazards management, edited by:
998 Agrawala, S., Organisation for Economic Cooperation and Development (OECD), Paris, France, 25-125, 2007.
- 999 Allen, M. R., and Ingram, W. J.: Constraints on future changes in climate and the hydrologic cycle, *Nature*, 419,
1000 224-232, 10.1038/nature01092, 2002.
- 1001 Ban, N., Schmidli, J., and Schär, C.: Heavy precipitation in a changing climate: Does short-term summer
1002 precipitation increase faster?, *Geophys Res Lett*, 42, 1165-1172, 10.1002/2014GL062588, 2015.
- 1003 Beniston, M.: Climatic Change in Mountain Regions: A Review of Possible Impacts. *Clim Change*, 59, 5-31.
- 1004 Beniston, M.: Impacts of climatic change on water and associated economic activities in the Swiss Alps, *J Hydrol*,
1005 412, 291-296, 10.1016/j.jhydrol.2010.06.046, 2012.
- 1006 [Ceppi, P., Scherrer, S.C., Fischer, A.M., and Appenzeller, C.: Revisiting Swiss temperature trends 1959–2008, *Int*
1007 *J Climatol*, 32, 203-213, 10.1002/joc.2260, 2012.](#)
- 1008 CH2011: Swiss Climate Change Scenarios CH2011, published by C2SM, MeteoSwiss, ETH, NCCR Climate, and
1009 OcCC, Zurich, Switzerland, 88 pp, 2011.
- 1010 [Chimani, B., Böhm, R., Matulla, C., and Ganekind, M.: Development of a longterm dataset of solid/liquid
1011 precipitation, *Adv Sci Res*, 6, 39-43, 10.5194/asr-6-39-2011, 2011.](#)
- 1012 de Vries, H., Haarsma, R. J., Hazeleger, W.: On the future reduction of snowfall in western and central Europe.
1013 *Clim Dyn*, 41, 2319-2330, 10.1007/s00382-012-1583-x, 2013.
- 1014 de Vries, H., Lenderink, G., and van Meijgaard, E.: Future snowfall in western and central Europe projected with a
1015 high-resolution regional climate model ensemble, *Geophys Res Lett*, 41, 4294-4299, 10.1002/2014GL059724,
1016 2014.
- 1017 Deser, C., Knutti, R., Solomon, S. and Phillips, A. S.: Communication of the role of natural variability in future
1018 North American climate. *Nature Clim Change*, 2, 775-779, 2012.
- 1019 Elsasser, H. and Bürki, R.: Climate change as a threat to tourism in the Alps. *Climate Research*, 20, 253-257.
- 1020 Fischer, A. M., Keller, D. E., Liniger, M. A., Rajczak, J., Schär, C., and Appenzeller, C.: Projected changes in
1021 precipitation intensity and frequency in Switzerland: a multi-model perspective, *Int J Climatol*, 35, 3204-3219,
1022 10.1002/joc.4162, 2015.
- 1023 Fischer, E. M. and Knutti, R.: Observed heavy precipitation increase confirms theory and early models. *Nature*
1024 *Clim Change*, 6, 986-992, 10.1038/NCLIMATE3110, 2016.
- 1025 Frei, C. and Schär, C.: A precipitation climatology of the Alps from high-resolution rain-gauge observations, *Int J*
1026 *Climatol*, 18, 873-900, 10.1002/(Sici)1097-0088(19980630)18:8<873::Aid-Joc255>3.0.Co;2-9, 1998.
- 1027 Frei, C., Christensen, J. H., Déqué, M., Jacob, D., Jones, R. G., and Vidale, P. L.: Daily precipitation statistics in
1028 regional climate models: Evaluation and intercomparison for the European Alps, *J Geophys Res-Atmos*, 108,
1029 10.1029/2002jd002287, 2003.
- 1030 Frei, C.: Interpolation of temperature in a mountainous region using nonlinear profiles and non-Euclidean
1031 distances, *Int J Climatol*, 34, 1585-1605, 10.1002/joc.3786, 2014.
- 1032 Giorgi, F.: Simulation of regional climate using a limited area model nested in a general circulation model, *J*
1033 *Climate*, 3, 941-963, 1990.
- 1034 Giorgi, F., Jones, C., and Asrar, G. R.: Addressing climate information needs at the regional level: the CORDEX
1035 framework, *World Meteorological Organization (WMO) Bulletin*, 58, 175, 2009.
- 1036 Giorgi, F., Torma, C., Coppola, E., Ban, N., Schär, C., and Somot, S.: Enhanced summer convective rainfall at
1037 Alpine high elevations in response to climate warming, *Nat Geo*, 9, 584-589, 10.1038/ngeo2761, 2016.
- 1038 Gobiet, A., Kotlarski, S., Beniston, M., Heinrich, G., Rajczak, J., and Stoffel, M.: 21st century climate change in
1039 the European Alps - A review, *Science of the Total Environment*, 493, 1138-1151,
1040 10.1016/j.scitotenv.2013.07.050, 2014.
- 1041 [Grünewald, T., and Lehning, M.: Are flat-field snow depth measurements representative? A comparison of
1042 selected index sites with areal snow depth measurements at the small catchment scale, *Hydrol Processes*, 29,
1043 1717-1728, 10.1002/hyp.10295, 2015.](#)

- 1044 Hantel, M., Maurer, C., and Mayer, D.: The snowline climate of the Alps 1961–2010. *Theor Appl Climatol*, 110,
1045 517, 10.1007/s00704-012-0688-9, 2012.
- 1046 Hawkins, E., and Sutton, R.: The Potential to Narrow Uncertainty in Regional Climate Predictions, *B Am Meteorol*
1047 *Soc*, 90, 1095–+, 10.1175/2009BAMS2607.1, 2009.
- 1048 Haylock, M.R., Hofstra, N., Klein Tank, A.M.G., Klok, E.J., Jones, P.D., and New, M.: A European daily high-
1049 resolution gridded data set of surface temperature and precipitation for 1950–2006, *J Geophys Res*, 113,
1050 D20119, 10.1029/2008JD010201.
- 1051 Held, I. M., and Soden, B. J.: Robust responses of the hydrological cycle to global warming, *J Climate*, 19, 5686-
1052 5699, 10.1175/Jcli3990.1, 2006.
- 1053 IPCC: Climate Change 2013: The Physical Science Basis. Contribution of Working Group I to the Fifth
1054 Assessment Report of the Intergovernmental Panel on Climate Change, Cambridge University Press, Cambridge,
1055 United Kingdom and New York, NY, USA, 1535 pp., 2013.
- 1056 Isotta, F. A., Frei, C., Weilguni, V., Tadic, M. P., Lassegues, P., Rudolf, B., Pavan, V., Cacciamani, C., Antolini,
1057 G., Ratto, S. M., Munari, M., Micheletti, S., Bonati, V., Lussana, C., Ronchi, C., Panettieri, E., Marigo, G., and
1058 Vertacnik, G.: The climate of daily precipitation in the Alps: development and analysis of a high-resolution grid
1059 dataset from pan-Alpine rain-gauge data, *Int J Climatol*, 34, 1657-1675, 10.1002/joc.3794, 2014.
- 1060 Jacob, D., Petersen, J., Eggert, B., Alias, A., Christensen, O. B., Bouwer, L. M., Braun, A., Colette, A., Déqué, M.,
1061 Georgievski, G., Georgopoulou, E., Gobiet, A., Menut, L., Nikulin, G., Haensler, A., Hempelmann, N., Jones, C.,
1062 Keuler, K., Kovats, S., Kröner, N., Kotlarski, S., Kriegsman, A., Martin, E., van Meijgaard, E., Moseley, C.,
1063 Pfeifer, S., Preuschmann, S., Radermacher, C., Radtke, K., Rechid, D., Rounsevell, M., Samuelsson, P., Somot,
1064 S., Soussana, J. F., Teichmann, C., Valentini, R., Vautard, R., Weber, B., and Yiou, P.: EURO-CORDEX: new
1065 high-resolution climate change projections for European impact research, *Reg Environ Change*, 14, 563-578,
1066 10.1007/s10113-013-0499-2, 2014.
- 1067 Keller, D. E., Fischer, A. M., Liniger, M. A., Appenzeller, C. and Knutti, R.: Testing a weather generator for
1068 downscaling climate change projections over Switzerland. *Int J Climatol*, doi:10.1002/joc.4750, 2016.
- 1069 Kienzle, S. W.: A new temperature based method to separate rain and snow, *Hydrol Process*, 22, 5067-5085,
1070 10.1002/hyp.7131, 2008.
- 1071 [Kotlarski, S., Bosshard, T., Lüthi, D., Pall, P., and Schär, C.: Elevation gradients of European climate change in
1072 the regional climate model COSMO-CLM. *Clim Change*, 112, 189-215, 10.1007/s10584-011-0195-5, 2012.](#)
- 1073 Kotlarski, S., Keuler, K., Christensen, O. B., Colette, A., Deque, M., Gobiet, A., Goergen, K., Jacob, D., Luthi, D.,
1074 van Meijgaard, E., Nikulin, G., Schar, C., Teichmann, C., Vautard, R., Warrach-Sagi, K., and Wulfmeyer, V.:
1075 Regional climate modeling on European scales: a joint standard evaluation of the EURO-CORDEX RCM
1076 ensemble, *Geosci Model Dev*, 7, 1297-1333, 10.5194/gmd-7-1297-2014, 2014.
- 1077 Kotlarski, S., Lüthi, D., and Schär, C.: The elevation dependency of 21st century European climate change: an
1078 RCM ensemble perspective, *Int J Climatol*, 35, 3902-3920, 10.1002/joc.4254, 2015.
- 1079 Krasting, J. P., Broccoli, A. J., Dixon, K. W., and Lanzante, J. R.: Future Changes in Northern Hemisphere
1080 Snowfall. *J Clim*, 26, 7813-7828, 10.1175/JCLI-D-12-00832.1, 2013.
- 1081 Laternser, M., and Schneebeli, M.: Long-term snow climate trends of the Swiss Alps (1931-99), *Int J Climatol*, 23,
1082 733-750, 10.1002/joc.912, 2003.
- 1083 Marty, C.: Regime shift of snow days in Switzerland, *Geophys Res Lett*, 35, 10.1029/2008gl033998, 2008.
- 1084 Marty, C., and Blanchet, J.: Long-term changes in annual maximum snow depth and snowfall in Switzerland
1085 based on extreme value statistics, *Climatic Change*, 111, 705-721, 2011.
- 1086 McAfee, S. A., Walsh, J., and Rupp, T. S.: Statistically downscaled projections of snow/rain partitioning for
1087 Alaska, *Hydrol Process*, 28, 3930-3946, 10.1002/hyp.9934, 2014.
- 1088 [MeteoSchweiz: Klimareport 2015. Bundesamt für Meteorologie und Klimatologie MeteoSchweiz, Zürich.](#)
- 1089 MeteoSwiss: Daily Precipitation (final analysis): RhiresD:
1090 [www.meteoswiss.admin.ch/content/dam/meteoswiss/de/service-und-publikationen/produkt/raeumliche-daten-](http://www.meteoswiss.admin.ch/content/dam/meteoswiss/de/service-und-publikationen/produkt/raeumliche-daten-niederschlag/doc/ProdDoc_RhiresD.pdf)
1091 [niederschlag/doc/ProdDoc_RhiresD.pdf](http://www.meteoswiss.admin.ch/content/dam/meteoswiss/de/service-und-publikationen/produkt/raeumliche-daten-niederschlag/doc/ProdDoc_RhiresD.pdf), access: 10.01.2017, 2013a.
- 1092 MeteoSwiss: Daily Mean, Minimum and Maximum Temperature: TabsD, TminD, TmaxD:
1093 [www.meteoswiss.admin.ch/content/dam/meteoswiss/de/service-und-publikationen/produkt/raeumliche-daten-](http://www.meteoswiss.admin.ch/content/dam/meteoswiss/de/service-und-publikationen/produkt/raeumliche-daten-temperatur/doc/ProdDoc_TabsD.pdf)
1094 [temperatur/doc/ProdDoc_TabsD.pdf](http://www.meteoswiss.admin.ch/content/dam/meteoswiss/de/service-und-publikationen/produkt/raeumliche-daten-temperatur/doc/ProdDoc_TabsD.pdf), access: 10.01.2017, 2013b.
- 1095 Moss, R. H., Edmonds, J. A., Hibbard, K. A., Manning, M. R., Rose, S. K., van Vuuren, D. P., Carter, T. R., Emori,
1096 S., Kainuma, M., Kram, T., Meehl, G. A., Mitchell, J. F. B., Nakicenovic, N., Riahi, K., Smith, S. J., Stouffer, R. J.,
1097 Thomson, A. M., Weyant, J. P., and Wilbanks, T. J.: The next generation of scenarios for climate change research
1098 and assessment, *Nature*, 463, 747-756, 10.1038/nature08823, 2010.

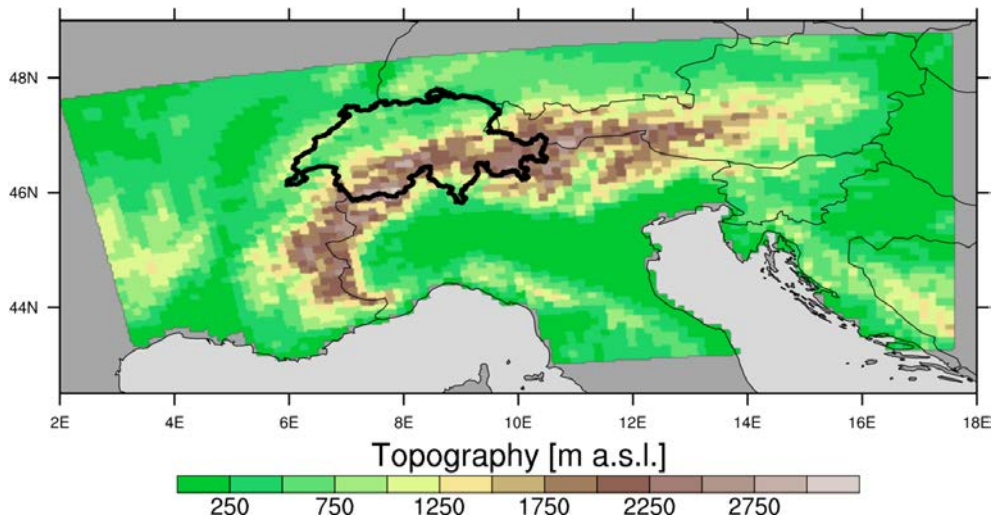
- 1099 Neff, E. L.: How Much Rain Does a Rain Gauge Gauge, *J Hydrol*, 35, 213-220, 10.1016/0022-1694(77)90001-4,
1100 1977.
- 1101 O'Gorman, P. A.: Contrasting responses of mean and extreme snowfall to climate change, *Nature*, 512, 416-
1102 U401, 10.1038/nature13625, 2014.
- 1103 Piazza, M., Boé, J., Terray, L., Pagé, C., Sanchez-Gomez, E., and Déqué, M.: Projected 21st century snowfall
1104 changes over the French Alps and related uncertainties, *Climatic Change*, 122, 583-594, 10.1007/s10584-013-
1105 1017-8, 2014.
- 1106 Räisänen, J.: Twenty-first century changes in snowfall climate in Northern Europe in ENSEMBLES regional
1107 climate models, *Clim Dynam*, 46, 339-353, 10.1007/s00382-015-2587-0, 2016.
- 1108 Rajczak, J., Pall, P., and Schär, C.: Projections of extreme precipitation events in regional climate simulations for
1109 Europe and the Alpine Region, *J Geophys Res-Atmos*, 118, 3610-3626, 10.1002/jgrd.50297, 2013.
- 1110 Rajczak, J., Kotlarski, S., and Schär, C.: Does Quantile Mapping of Simulated Precipitation Correct for Biases in
1111 Transition Probabilities and Spell Lengths?, *J Climate*, 29, 1605-1615, 10.1175/Jcli-D-15-0162.1, 2016.
- 1112 Rajczak, J. and Schär, C.: Projections of future precipitation extremes over Europe: A multi-model assessment of
1113 climate simulations. In preparation.
- 1114 Richards, F. J.: A Flexible Growth Function for Empirical Use, *J Exp Bot*, 10, 290-300, 10.1093/Jxb/10.2.290,
1115 1959.
- 1116 Rummukainen, M.: State-of-the-art with regional climate models, *Wiley Interdisciplinary Reviews-Climate Change*,
1117 1, 82-96, 10.1002/wcc.8, 2010.
- 1118 Schär, C., Ban, N., Fischer, E. M., Rajczak, J., Schmidli, J., Frei, C., Giorgi, F., Karl, T. R., Kendon, E. J., Tank, A.
1119 M. G. K., O'Gorman, P. A., Sillmann, J., Zhang, X. B., and Zwiers, F. W.: Percentile indices for assessing changes
1120 in heavy precipitation events, *Climatic Change*, 137, 201-216, 10.1007/s10584-016-1669-2, 2016.
- 1121 Scherrer, S. C., Appenzeller, C., and Laternser, M.: Trends in Swiss Alpine snow days: The role of local- and
1122 large-scale climate variability, *Geophys Res Lett*, 31, 10.1029/2004gl020255, 2004.
- 1123 Schmidli, J., Frei, C., and Vidale, P. L.: Downscaling from GCM precipitation: A benchmark for dynamical and
1124 statistical downscaling methods, *Int J Climatol*, 26, 679-689, 10.1002/joc.1287, 2006.
- 1125 Schmucki, E., Marty, C., Fierz, C., and Lehning, M.: Simulations of 21st century snow response to climate change
1126 in Switzerland from a set of RCMs, *Int J Climatol*, 35, 3262-3273, 10.1002/joc.4205, 2015a.
- 1127 Schmucki, E., Marty, C., Fierz, C., Weingartner, R. and Lehning, M.: Impact of climate change in Switzerland on
1128 socioeconomic snow indices, *Theor Appl Climatol*, in press, 10.1007/s00704-015-1676-7, 2015b.
- 1129 Serquet, G., Marty, C., and Rebetez, M.: Monthly trends and the corresponding altitudinal shift in the
1130 snowfall/precipitation day ratio, *Theor Appl Climatol*, 114, 437-444, 10.1007/s00704-013-0847-7, 2013.
- 1131 Der Niederschlag in der Schweiz, Geographisches Institut der Eidgenössischen Technischen Hochschule in
1132 Zürich, Abteilung Hydrologie, Zurich, Switzerland, 1985.
- 1133 SFOE, Hydropower: <http://www.bfe.admin.ch/themen/00490/00491/index.html?lang=en>, access: 16.09.2016,
1134 2014.
- 1135 Smiatek, G., Kunstmann, H., and Senatore, A.: EURO-CORDEX regional climate model analysis for the Greater
1136 Alpine Region: Performance and expected future change, *J Geophys Res-Atmos*, 121, 7710-7728,
1137 10.1002/2015JD024727, 2016.
- 1138 Soncini, A., and Bocchiola, D.: Assessment of future snowfall regimes within the Italian Alps using general
1139 circulation models, *Cold Reg Sci Technol*, 68, 113-123, 10.1016/j.coldregions.2011.06.011, 2011.
- 1140 Steger, C., Kotlarski, S., Jonas, T., and Schär, C.: Alpine snow cover in a changing climate: a regional climate
1141 model perspective, *Clim Dynam*, 41, 735-754, 10.1007/s00382-012-1545-3, 2013.
- 1142 Techel, F., Stucki, T., Margreth, S., Marty, C., and Winkler, K.: Schnee und Lawinen in den Schweizer Alpen.
1143 Hydrologisches Jahr 2013/14, WSL-Institut für Schnee- und Lawinenforschung SLF, Birmensdorf, Switzerland,
1144 2015.
- 1145 Terzago, S., von Hardenberg, J., Palazzi, E., and Provenzale, A.: Snow water equivalent in the Alps as seen by
1146 gridded datasets, CMIP5 and CORDEX climate models. *The Cryosphere Discussion*, 10.5194/tc-2016-280, 2017.
- 1147 Torma, C., Giorgi, F., and Coppola, E.: Added value of regional climate modeling over areas characterized by
1148 complex terrain Precipitation over the Alps, *J Geophys Res-Atmos*, 120, 3957-3972, 10.1002/2014JD022781,
1149 2015.
- 1150 Vautard, R., Gobiet, A., Jacob, D., Belda, M., Colette, A., Déqué, M., Fernandez, J., Garcia-Diez, M., Goergen,
1151 K., Guttler, I., Halenka, T., Karacostas, T., Katragkou, E., Keuler, K., Kotlarski, S., Mayer, S., van Meijgaard, E.,
1152 Nikulin, G., Patarcic, M., Scinocca, J., Sobolowski, S., Suklitsch, M., Teichmann, C., Warrach-Sagi, K.,
1153 Wulfmeyer, V., and Yiou, P.: The simulation of European heat waves from an ensemble of regional climate
1154 models within the EURO-CORDEX project, *Clim Dynam*, 41, 2555-2575, 10.1007/s00382-013-1714-z, 2013.

- 1155 Weingartner, R., Schädler, B., and Hänggi, P.: Auswirkungen der Klimaänderung auf die schweizerische
1156 Wasserkraftnutzung, *Geographica Helvetica*, 68, 239-248, 2013.
- 1157 Yang, D. Q., Elomaa, E., Tuominen, A., Aaltonen, A., Goodison, B., Gunther, T., Golubev, V., Sevruk, B.,
1158 Madsen, H., and Milkovic, J.: Wind-induced precipitation undercatch of the Hellmann gauges, *Nord Hydrol*, 30,
1159 57-80, 1999.
- 1160 Zubler, E. M., Scherrer, S. C., Croci-Maspoli, M., Liniger, M. A., and Appenzeller, C.: Key climate indices in
1161 Switzerland; expected changes in a future climate, *Climatic Change*, 123, 255-271, 10.1007/s10584-013-1041-8,
1162 2014.
- 1163 Zubler, E. M., Fischer, A. M., Liniger, M. A., and Schlegel, T.: Auftausalzverbrauch im Klimawandel, MeteoSwiss,
1164 Zurich, Switzerland, Fachbericht 253, 2015.
- 1165

1166 **Figures**

1167

1168

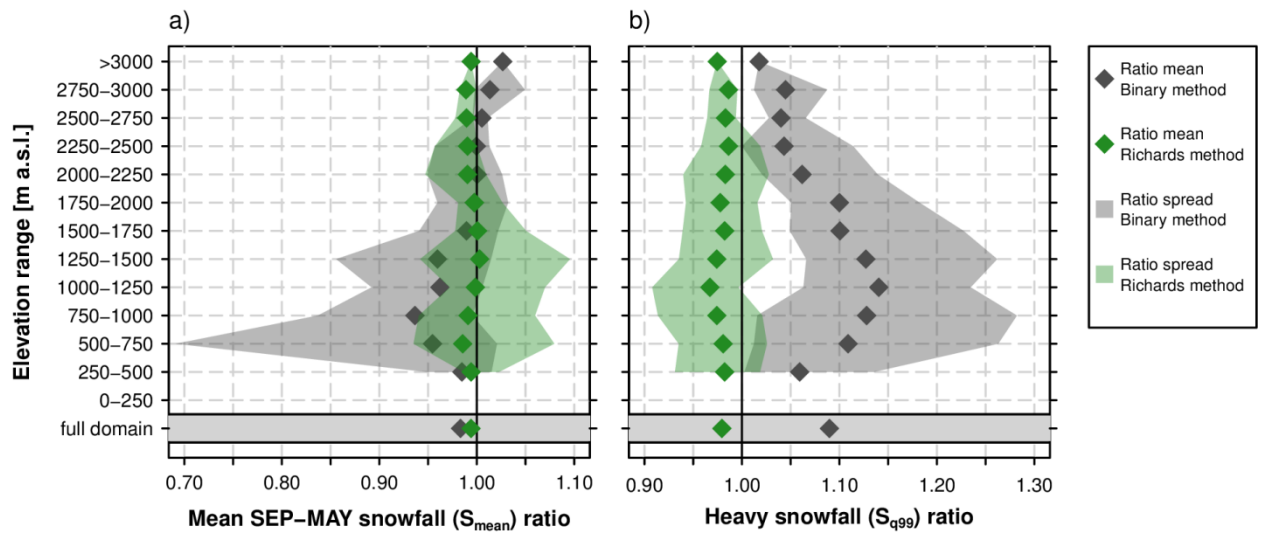


1169

1170

1171 **Figure 1** GTOPO30 topography (<https://ita.cr.usgs.gov/GTOPO30>) aggregated to the at-EUR-11 (0.11°) RCM
1172 grid. resolution of The coloured area shows the Alpine domain used for the assessment of snowfall projections.
1173 The bold black outline marks the Swiss sub-domain used for the assessment of the bias adjustment~~correction~~
1174 approach.

1175

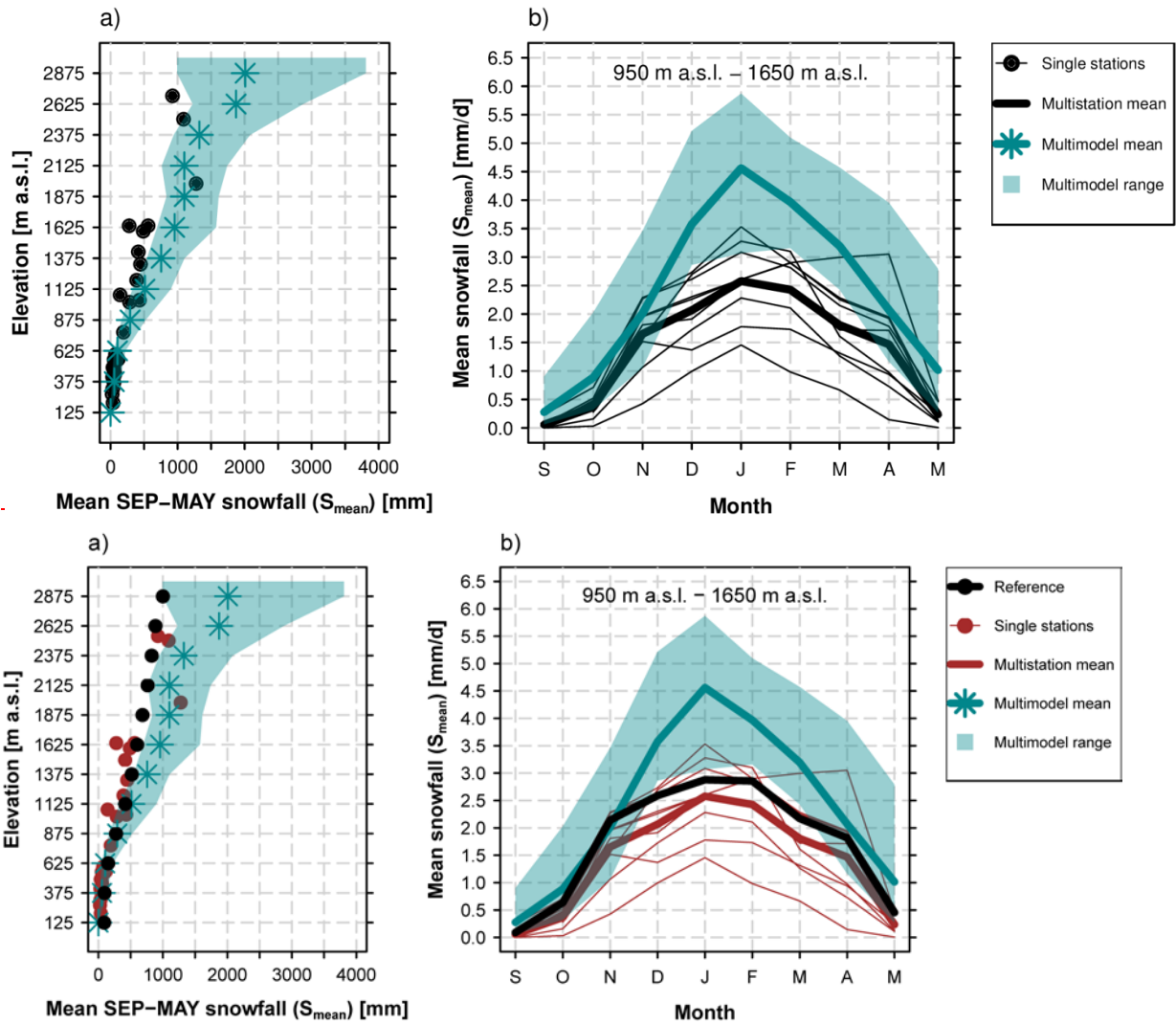


1176

1177

1178 **Figure 2** Snowfall ratios for the Binary and Richards snow fractionation method (ratio between the snowfall of the
 1179 respective method and the ~~full-subgrid-snow-representation~~ Subgrid method). The ratios are valid at the coarse-
 1180 resolution grid (12 km). a) Ratios for mean snowfall, S_{mean} . b) Ratios for heavy snowfall, S_{q99} . Ratio means were
 1181 derived after averaging the corresponding snowfall index for 250 m elevation intervals in Switzerland while the
 1182 ratio spread represents the minimum and maximum grid point-based ratios in the corresponding elevation
 1183 interval. This analysis is entirely based on the observational data sets TabsD and RhiresD.

1184

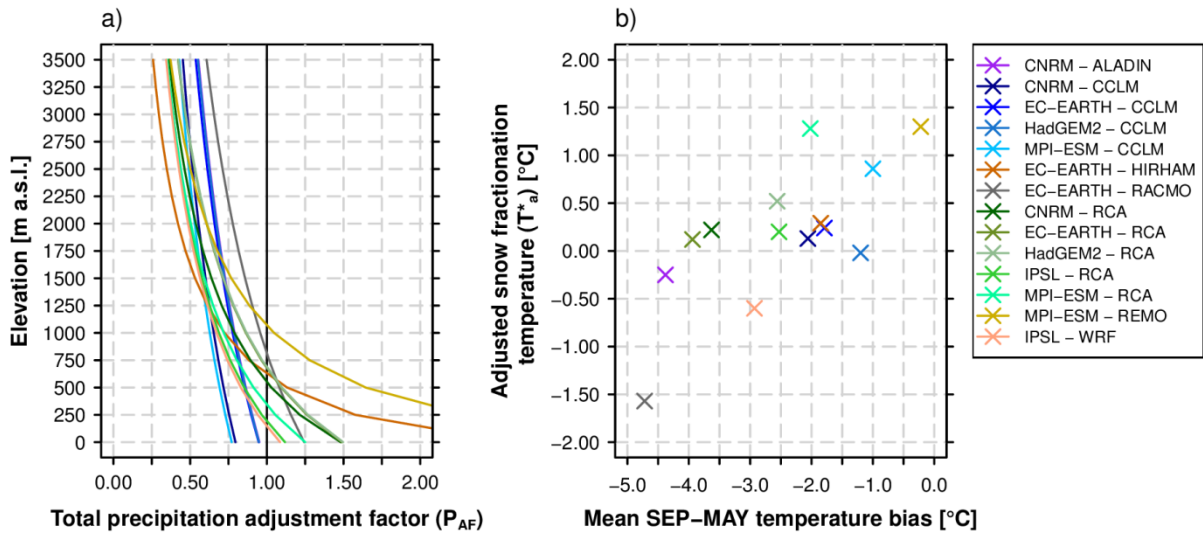


1185

1186

1187 **Figure 3** Comparison of measured fresh snow sums of 29 MeteoSwiss stations (red) against vs. simulated RCM
 1188 raw snowfall in Switzerland (green) and against the 2 km reference snowfall grid obtained by employing the
 1189 Subgrid method (black) in the EVAL period 1971-2005. a) Mean September – May snowfall vs. elevation. Both
 1190 the simulation data (green) and the reference data (black) are based on the spatio-temporal mean of 250 m
 1191 elevation ranges and plotted at the mean elevation of the corresponding interval. b) Seasonal September-May
 1192 snowfall cycle for the elevation interval 950 m a.s.l. to 1650 m a.s.l.. Simulated multi-model means and spreads
 1193 are based on a subset of 9 EURO-CORDEX simulations providing raw snowfall as output variable (see Tab. 1).

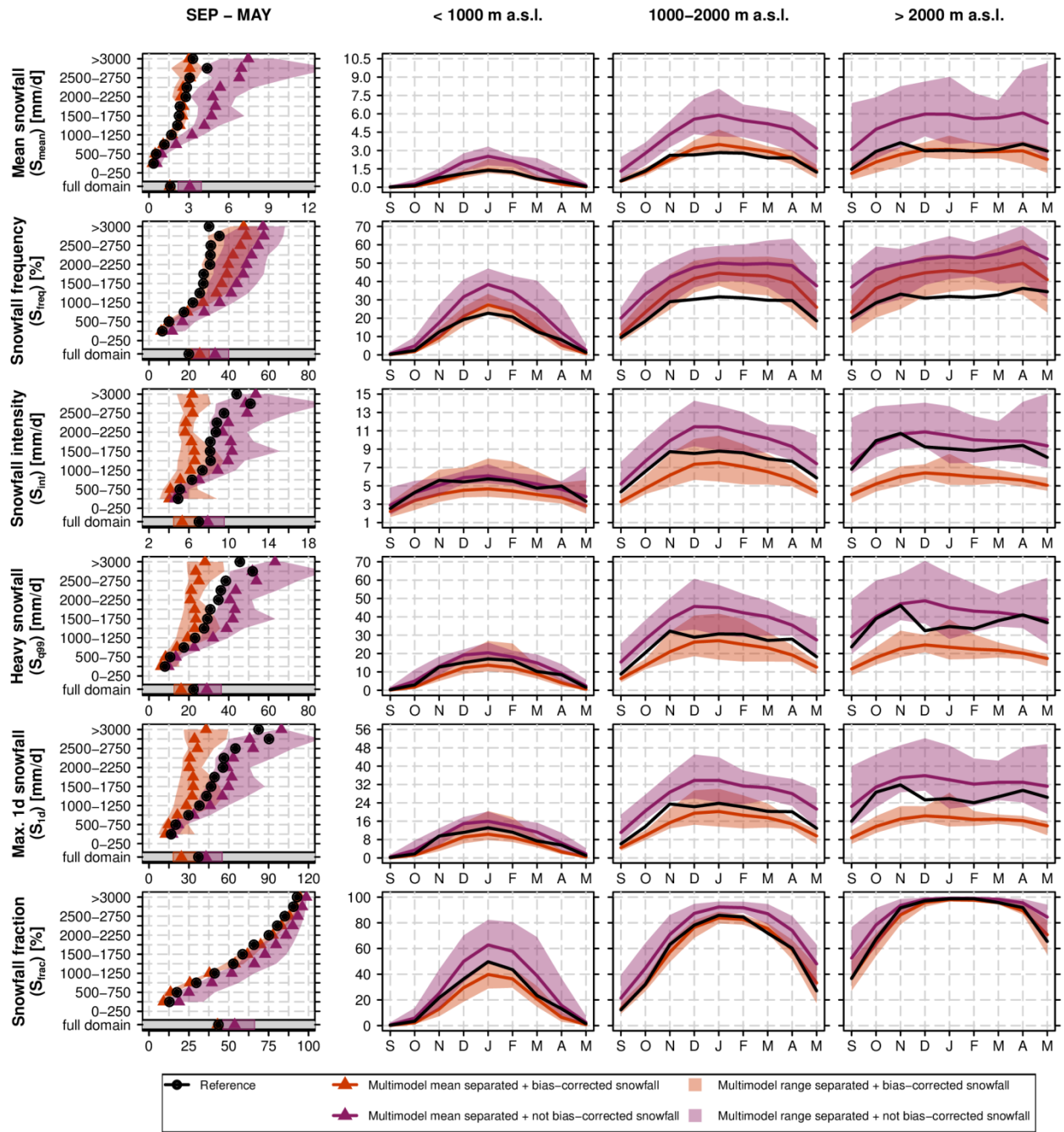
1194



1195

1196

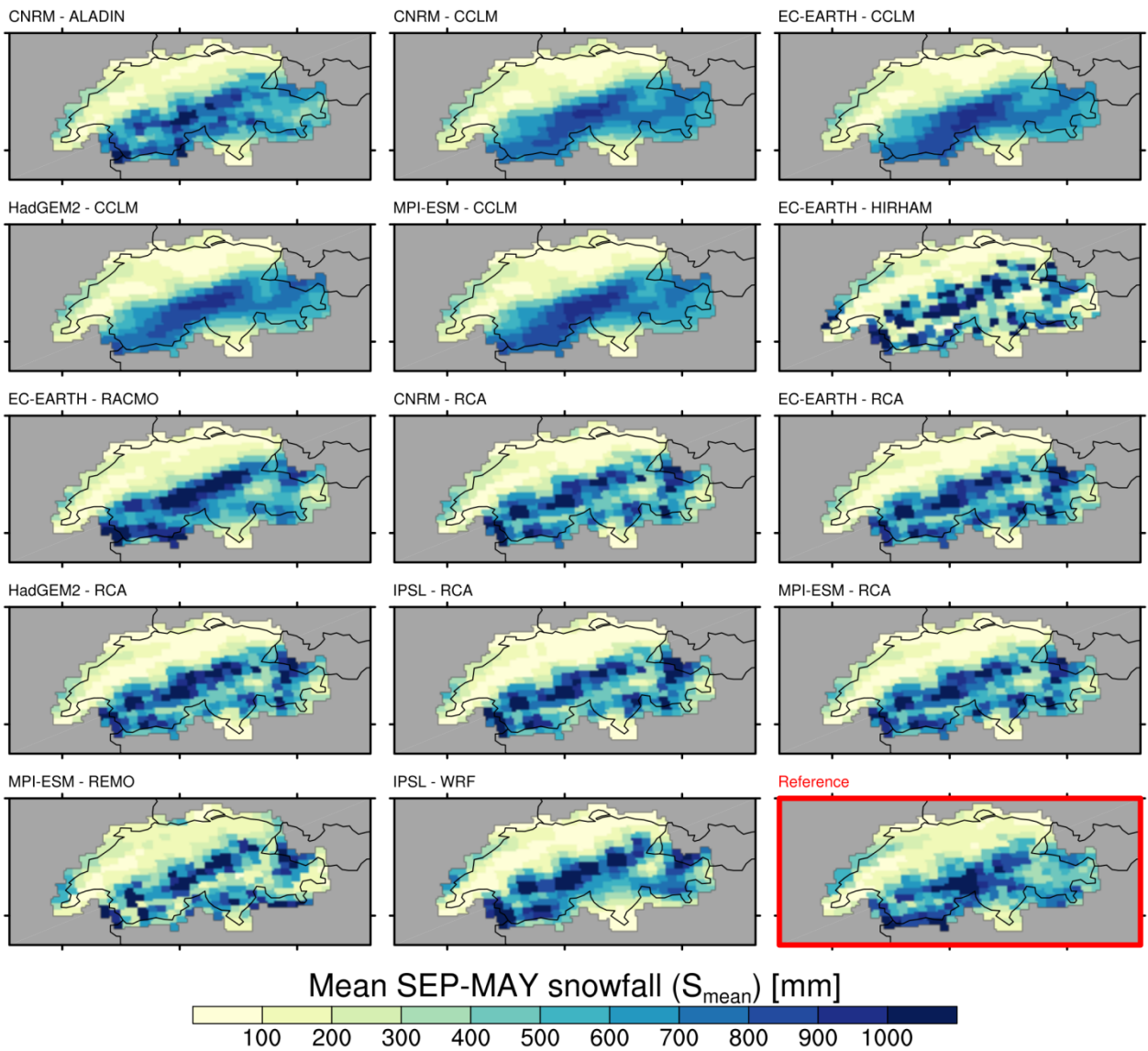
1197 | **Figure 4** ~~Bias correction and adjustment factors~~ Overview on bias adjustment. a) Elevation-dependent total
 1198 precipitation adjustment factors, P_{AF} , for the 14 GCM-RCM chains (see Eq. 10). b) Scatterplot of mean September
 1199 to May temperature biases (RCM simulation minus observational analysis) vs. adjusted snow fractionation
 1200 temperatures, T^*_a .



1201
1202

1203 **Figure 5** Evaluation of snowfall indices in the EVAL period 1971-2005 for the 14 snowfall separated + bias-
 1204 corrected-adjusted ($RCM_{sep+bae}$) and 14 snowfall separated + not bias-corrected-adjusted ($RCM_{sep+nb_{ae}}$) RCM
 1205 simulations vs. observation-based reference. The first column shows the mean September-May snowfall index
 1206 statistics vs. elevation while the monthly snowfall indices (spatially averaged over the elevation intervals <1000
 1207 m a.s.l., 1000 m a.s.l.-2000 m a.s.l. and >2000 m a.s.l.) are displayed in columns 2-4.

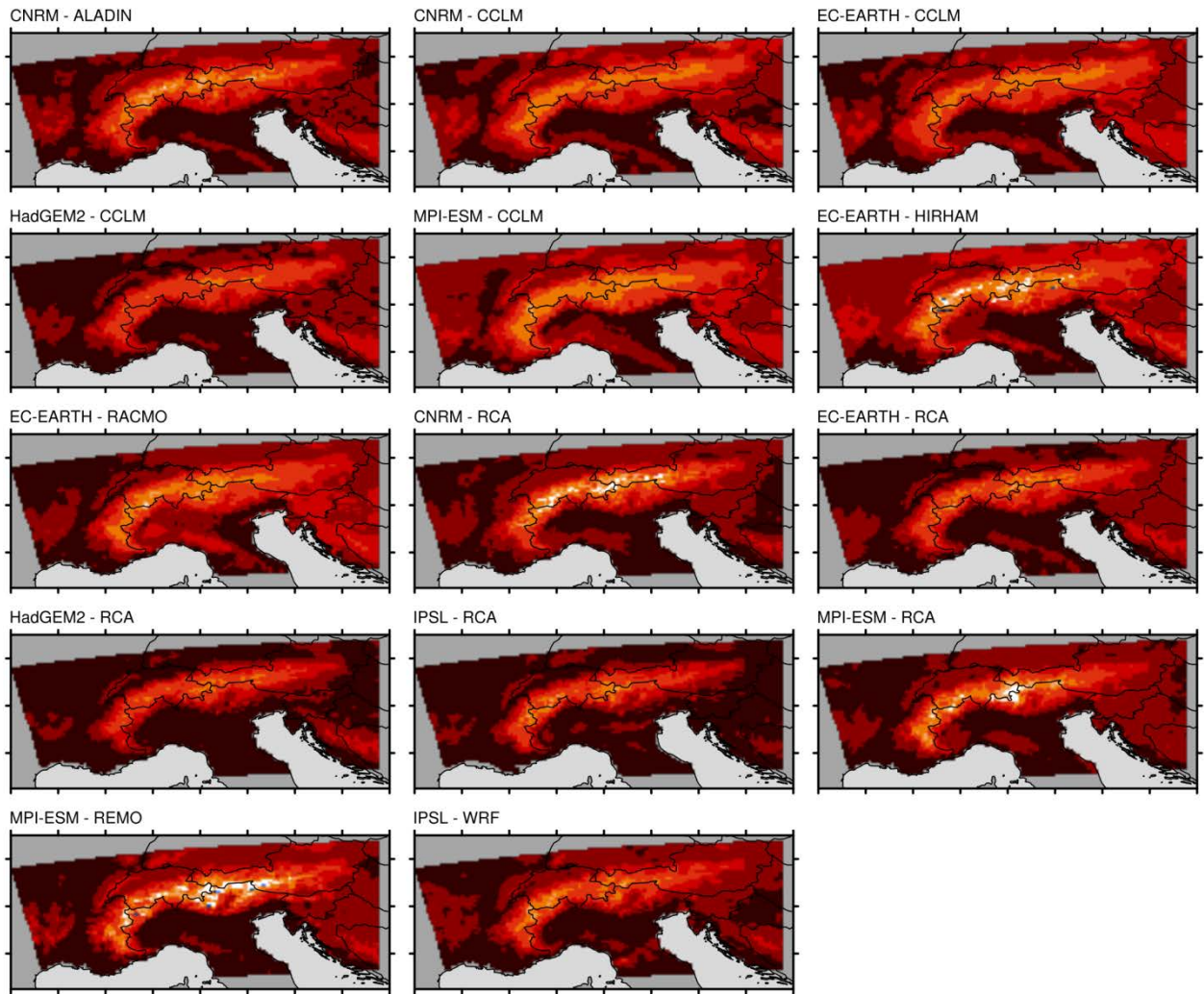
1208



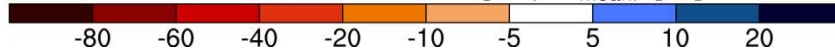
1209
1210

1211 **Figure 6** Spatial distribution of mean September-May snowfall, S_{mean} , in the EVAL period 1971-2005 and for the
 1212 | 14 snowfall separated + bias-~~corrected~~-adjusted RCM simulations ($\text{RCM}_{\text{sep}+\text{bae}}$). In the lower right panel, the map
 1213 of the observation-based reference is shown.

1214



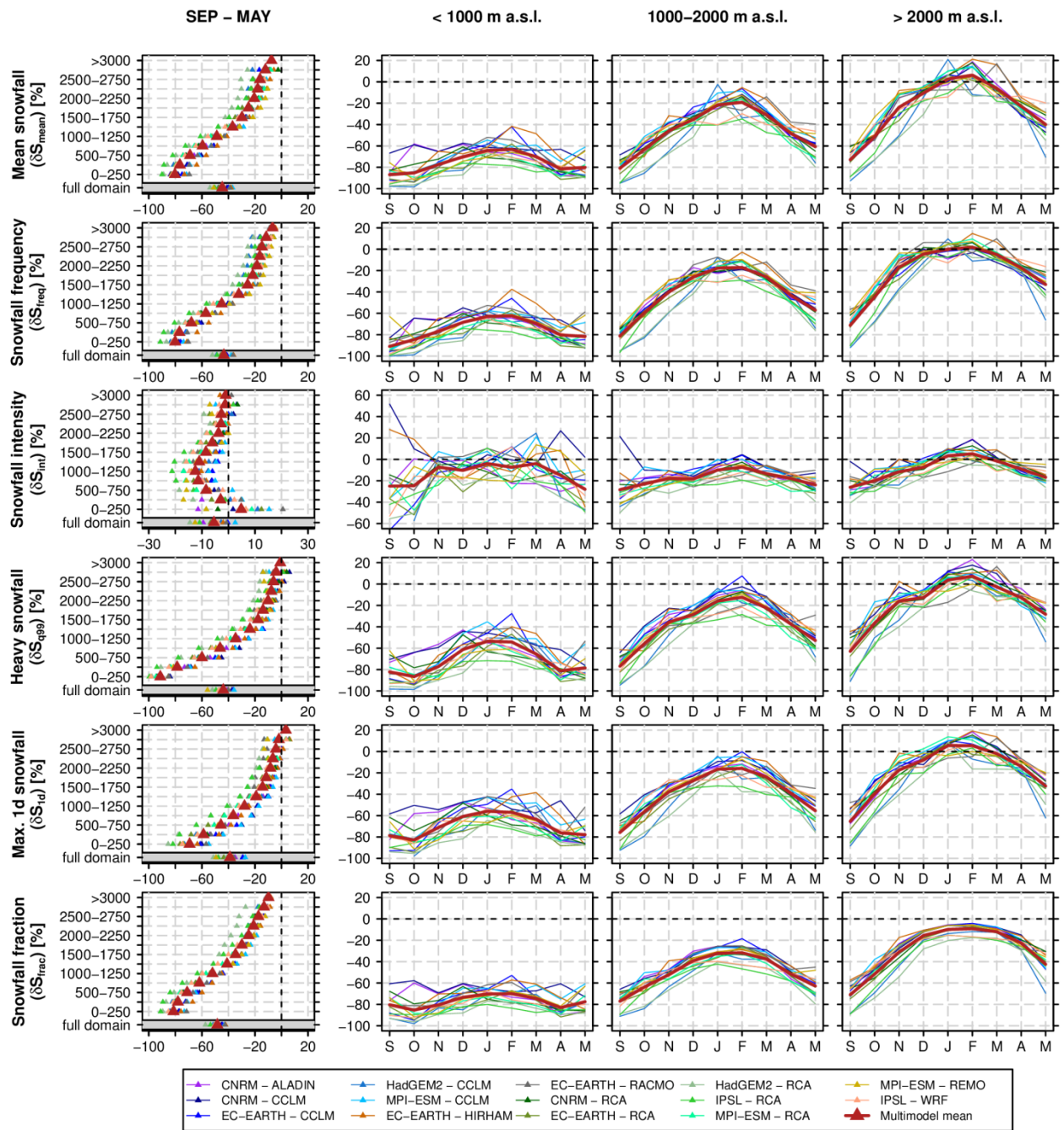
Mean SEP-MAY snowfall change (δS_{mean}) [%], RCP8.5



1215
1216

1217 **Figure 7** Spatial distribution of relative changes (SCEN period 2070-2099 with respect to CTRL period 1981-
1218 2010) in mean September-May snowfall, δS_{mean} , for RCP8.5 and for the 14 snowfall separated + bias_~~corrected~~
1219 adjusted RCM simulations ($\text{RCM}_{\text{sep+b3e}}$). For RCP4.5, see Fig. S65.

1220



1221

1222

1223

1224

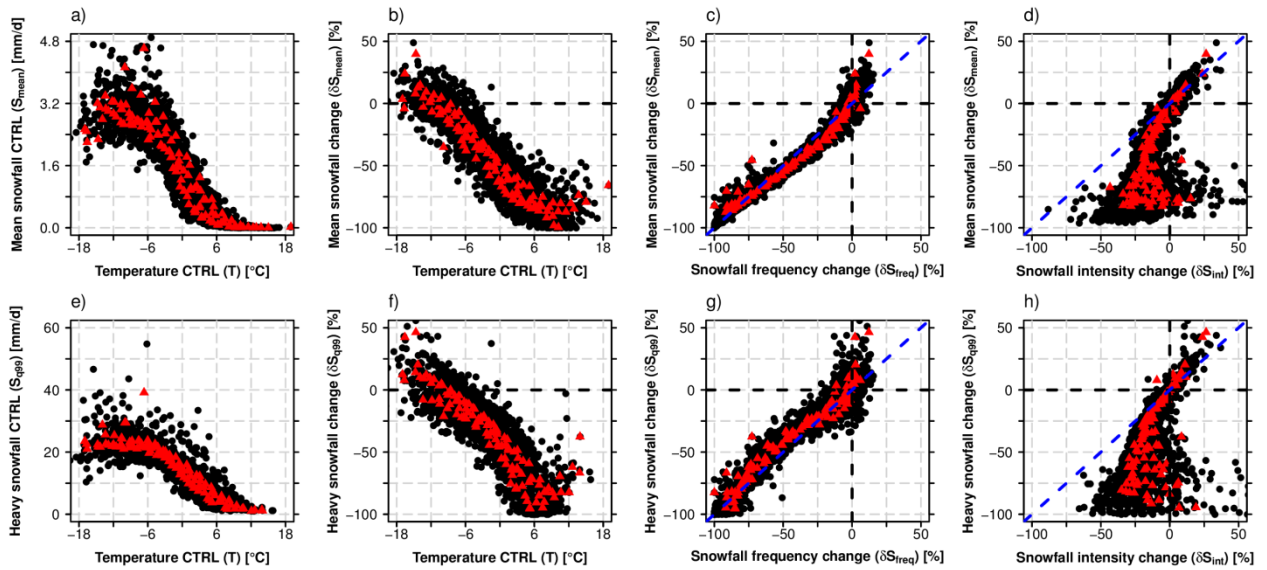
1225

1226

1227

1228

Figure 8 Relative changes (SCEN period 2070-2099 with respect to CTRL period 1981-2010) of snowfall indices based on the 14 snowfall separated + bias-corrected-adjusted RCM simulations (RCM_{sep+bc}) for RCP8.5. The first column shows the mean September-May snowfall index statistics vs. elevation while monthly snowfall index changes (spatially averaged over the elevation intervals <1000 m.a.s.l., 1000 m a.s.l.-2000 m a.s.l. and >2000 m a.s.l.) are displayed in columns 2-4.



1229

1230

1231

Figure 9 Intercomparison of various snowfall indices and relationship with monthly mean temperature in CTRL.

1232

For each panel, the monthly mean statistics for each 250 m elevation interval and for each of the 14 individual

1233

GCM-RCM chains were derived (black circles). Red triangles denote the multi-model mean for a specific month

1234

and elevation interval. The monthly statistics were calculated by considering all grid points of the specific

1235

elevation intervals which are available for both variables in the corresponding scatterplot only (area consistency).

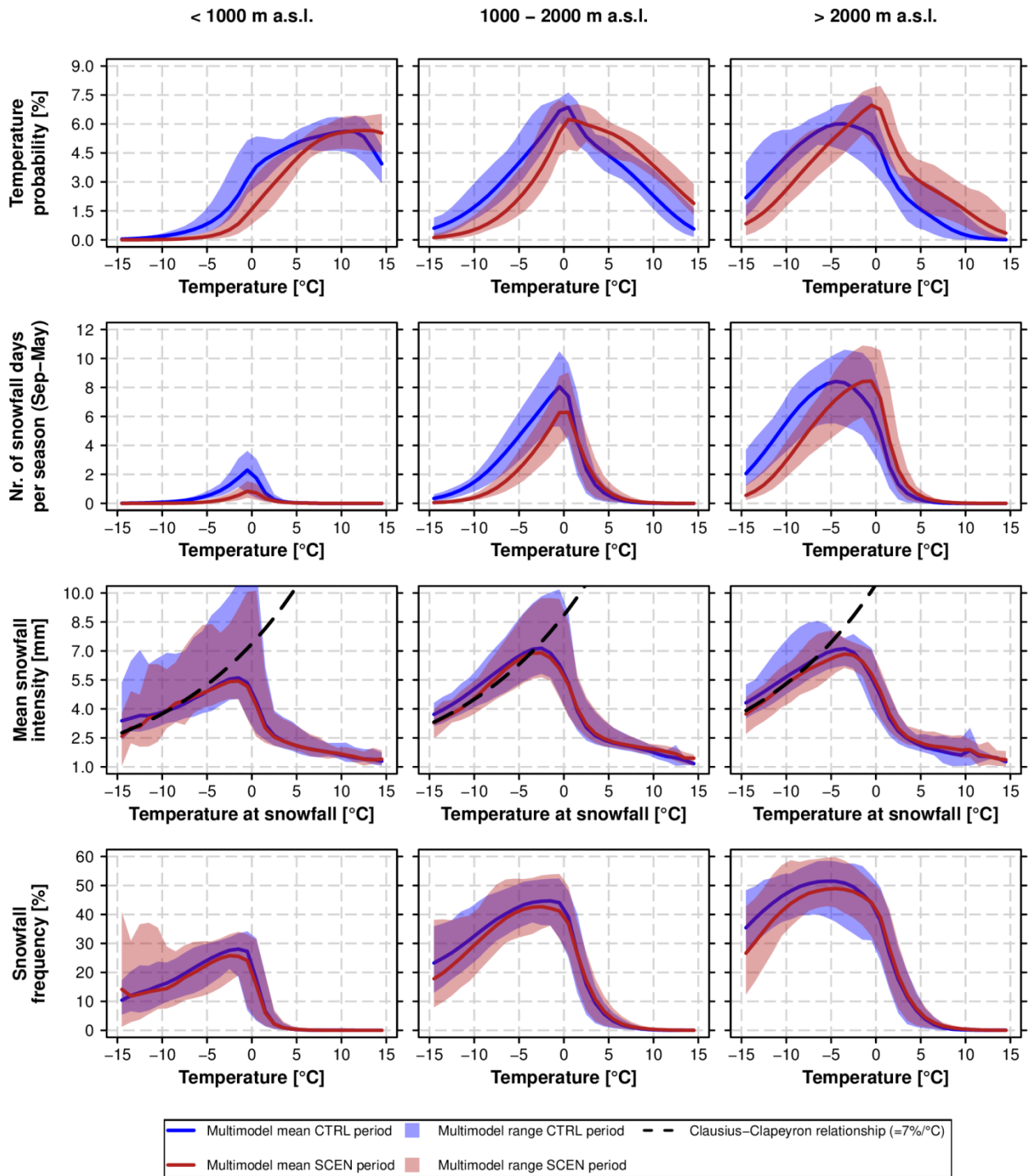
1236

The data were taken from the 14 snowfall separated + bias-corrected-adjusted (RCM_{sep+bias}) RCM simulations.

1237

Relative changes are based on the RCP8.5 driven simulations (SCEN 2070-2099 wrt. CTRL 1981-2010).

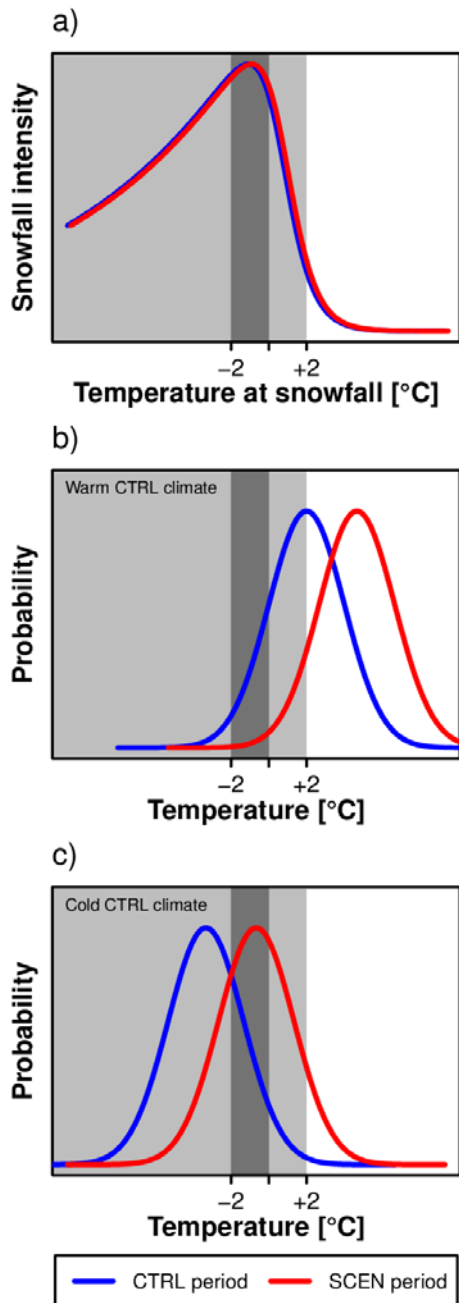
1238



1239

1240

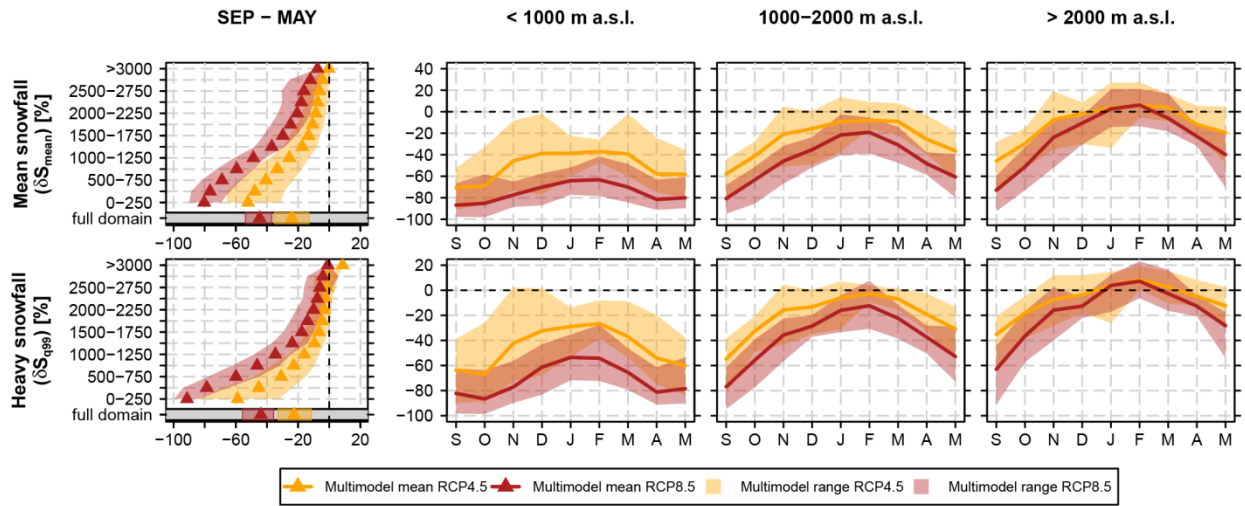
1241 **Figure 10** Comparison of temperature probability, snowfall probability and mean snowfall intensity for the CTRL
1242 period 1981-2010 and SCEN period 2070-2099 for RCP8.5. The analysis is based on data from the 14 snowfall
1243 separated + bias-corrected-adjusted RCM simulations (RCM_{sep+bae}). The top row depicts the PDF of the daily
1244 temperature distribution, while the second row shows the mean number of snowfall days between September and
1245 May, i.e., days with $S > 1 \text{ mm/d}$ (see Tab. 2), in a particular temperature interval. The third row represents the
1246 mean snowfall intensity, S_{int} , for a given snowfall temperature interval. In addition the Clausius-Clapeyron
1247 relationship, centred at the -10°C mean S_{int} for SCEN, is displayed by the black dashed line. PDFs and mean S_{int}
1248 were calculated by creating daily mean temperature bins of width 1°C .



1249
1250

1251 **Figure 11** Schematic illustration of the control of changes in snowfall intensity on changes in mean and extreme
 1252 snowfall. a) Relation between temperature and mean snowfall intensity. b) Daily temperature PDF for a warm
 1253 control climate (low elevations or transition seasons, i.e., beginning or end of winter). c) Daily temperature PDF
 1254 for a cold control climate (high elevations or mid-winter). The blue line denotes the historical CTRL period, the red
 1255 line the future SCEN period. The light grey shaded area represents the overall temperature interval at which
 1256 snowfall occurs, the dark grey shading shows the preferred temperature interval for heavy snowfall to occur.

1257



1258

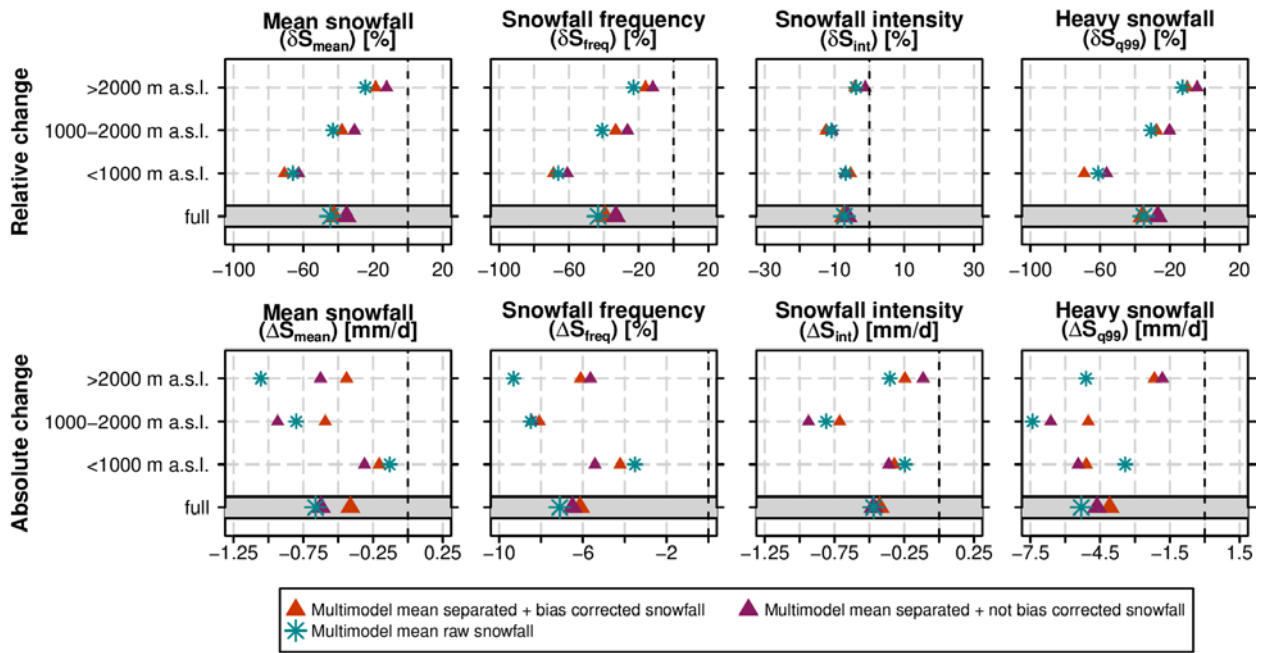
1259

1260

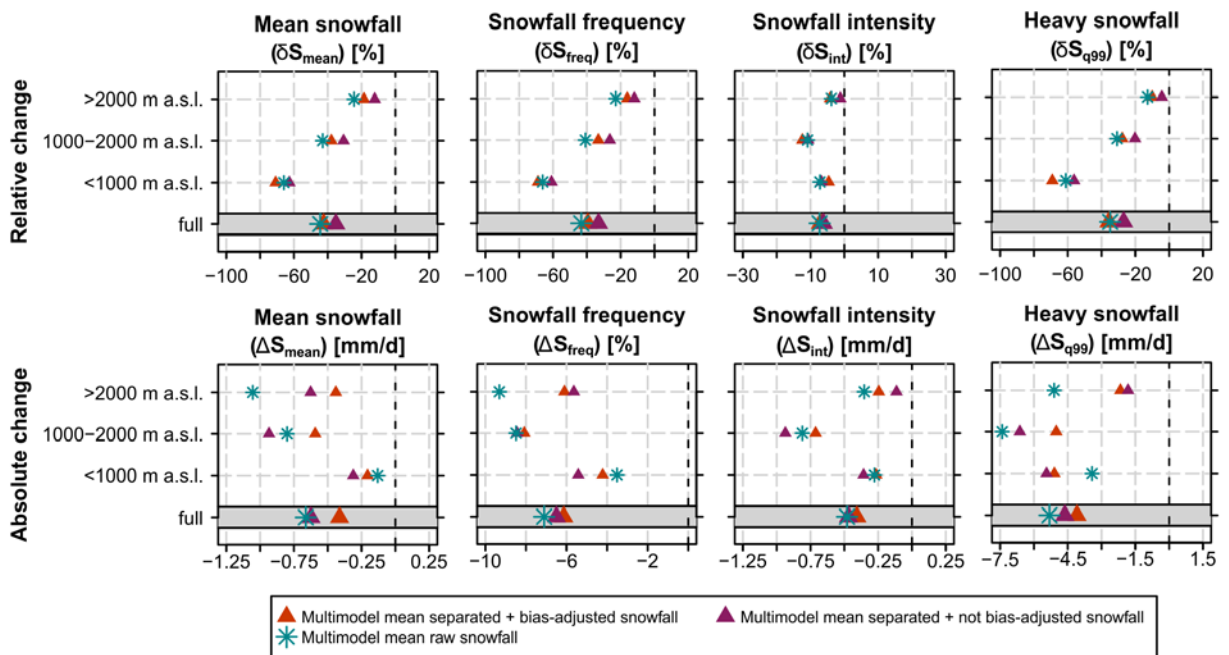
1261

Figure 12 Similar as Figure 8 but showing projected changes of mean snowfall, δS_{mean} , and heavy snowfall, δS_{q99} , for the emission scenarios RCP4.5 and 8.5. See Fig. S98 for the emission scenario uncertainty of the remaining four snowfall indices.

1262



1263
1264



1265
1266
1267
1268
1269
1270

Figure 13 Relative and absolute changes (SCEN period 2070-2099 with respect to CTRL period 1981-2010) of mean September-May snowfall indices based on a subset of 9 snowfall separated + bias-~~corrected~~-adjusted (RCM_{sep+bae}), 9 snowfall separated + not bias-~~corrected~~-adjusted (RCM_{sep+nbae}) and 9 raw snowfall RCM simulations (RCM_{raw}) for RCP8.5. Only RCM simulations providing raw snowfall as output variable (see Tab. 1) were used in this analysis.

1271

1272 **Tables**

1273

1274 | **Table 1** Overview on the 14 EURO-CORDEX simulations available for his study. The whole model set consists of
 1275 | seven RCMs driven by five different GCMs. All experiments were realized on a grid, covering the European
 1276 | domain, with a horizontal resolution of approximately 12.5 km (EUR-11) and were run for control RCP4.5 and
 1277 | RCP8.5 scenarios within the considered time periods of interest. A subset of 9 simulations provides raw snowfall,
 1278 | i.e., snowfall flux in kg/m²s, as output variable. For full institutional names the reader is referred to the official
 1279 | EURO-CORDEX website www.euro-cordex.net. Note that the EC-EARTH-driven experiments partly employ
 1280 | different realizations of the GCM run, i.e., explicitly sample the influence of internal climate variability in addition to
 1281 | model uncertainty.

RCM	GCM	Acronym	Institute ID	Raw snowfall output
ALADIN53	CNRM-CERFACS-CNRM-CM5	CNRM - ALADIN	CNRM	no
CCLM4-8-17	CNRM-CERFACS-CNRM-CM5	CNRM - CCLM	CLMcom/BTU	no
CCLM4-8-17	ICHEC-EC-EARTH	EC-EARTH - CCLM	CLMcom/BTU	no
CCLM4-8-17	MOHC-HadGEM2-ES	HadGEM2 - CCLM	CLMcom/ETH	no
CCLM4-8-17	MPI-M-MPI-ESM-LR	MPI-ESM - CCLM	CLMcom/BTU	no
HIRHAM5	ICHEC-EC-EARTH	EC-EARTH - HIRHAM	DMI	yes
RACMO22E	ICHEC-EC-EARTH	EC-EARTH - RACMO	KNMI	yes
RCA4	CNRM-CERFACS-CNRM-CM5	CNRM - RCA	SMHI	yes
RCA4	ICHEC-EC-EARTH	EC-EARTH - RCA	SMHI	yes
-RCA4	MOHC-HadGEM2-ES	HadGEM2 - RCA	SMHI	yes
RCA4	IPSL-IPSL-CM5A-MR	IPSL - RCA	SMHI	yes
RCA4	MPI-M-MPI-ESM-LR	MPI-ESM – RCA	SMHI	yes
REMO2009	MPI-M-MPI-ESM-LR	MPI-ESM – REMO*	MPI-CSC	yes
WRF331F	IPSL-IPSL-CM5A-MR	IPSL - WRF	IPSL-INERIS	yes

* r1i1p1 realisation

1282

1283

1284 **Table 2** Analysed snowfall indices. The last column indicates the threshold value in the CTRL period for
 1285 considering a grid cell in the climate changes analysis (grid cells with smaller values are skipped for the
 1286 respective analysis); first number: threshold for monthly analyses, second number: threshold for seasonal
 1287 analysis.

Index name	Acronym	Unit	Definition	Threshold for monthly / seasonal analysis
Mean snowfall	S_{mean}	mm	(Spatio-)temporal mean snowfall in mm snow water equivalent (only "mm" thereafter).	1 mm / 10 mm
Heavy snowfall	S_{q99}	mm/d	Grid point-based 99% all day snowfall percentile.	1 mm / 1 mm
Max. 1 day snowfall	S_{1d}	mm/d	Mean of each season's or month's maximum 1 day snowfall.	1 mm / 1 mm
Snowfall frequency	S_{freq}	%	Percentage of days with snowfall $S > 1$ mm/d within a specific time period.	1 % / 1 %
Snowfall intensity	S_{int}	mm/d	Mean snowfall intensity at days with snowfall $S > 1$ mm/d within a specific time period.	S_{freq} threshold passed
Snowfall fraction	S_{frac}	%	Percentage of total snowfall, S_{tot} , on total precipitation, P_{tot} , within a specific time period.	1 % / 1 %

1288
 1289
 1290
 1291